

# Formation of millisecond pulsars with CO white dwarf companions – II. Accretion, spin-up, true ages and comparison to MSPs with He white dwarf companions

T. M. Tauris,<sup>1,2</sup> N. Langer<sup>1</sup> and M. Kramer<sup>2,3</sup>

<sup>1</sup>*Argelander-Institut für Astronomie, Universität Bonn, Auf dem Hügel 71, 53121 Bonn, Germany*

<sup>2</sup>*Max-Planck-Institut für Radioastronomie, Auf dem Hügel 69, 53121 Bonn, Germany*

<sup>3</sup>*Jodrell Bank Centre for Astrophysics, University of Manchester, Oxford Rd, Manchester M13 9PL, UK*

Accepted 2012 June 3

## ABSTRACT

Millisecond pulsars are mainly characterised by their spin periods, B-fields and masses – quantities which are largely affected by previous interactions with a companion star in a binary system. In this paper, we investigate the formation mechanism of millisecond pulsars by considering the pulsar recycling process in both intermediate-mass X-ray binaries (IMXBs) and low-mass X-ray binaries (LMXBs). The IMXBs mainly lead to the formation of binary millisecond pulsars with a massive carbon-oxygen (CO) or an oxygen-neon-magnesium white dwarf (ONeMg WD) companion, whereas the LMXBs form recycled pulsars with a helium white dwarf (He WD) companion. We discuss the accretion physics leading to the spin-up line in the  $P\dot{P}$ -diagram and demonstrate that such a line cannot be uniquely defined. We derive a simple expression for the amount of accreted mass needed for any given pulsar to achieve its equilibrium spin and apply this to explain the observed differences of the spin distributions of recycled pulsars with different types of companions. From numerical calculations we present further evidence for significant loss of rotational energy in accreting X-ray millisecond pulsars in LMXBs during the Roche-lobe decoupling phase (Tauris 2012) and demonstrate that the same effect is negligible in IMXBs. We examine the recycling of pulsars with CO WD companions via Case BB Roche-lobe overflow (RLO) of naked helium stars in post common envelope binaries. We find that such pulsars typically accrete of the order  $0.002 - 0.007 M_{\odot}$  which is just about sufficient to explain their observed spin periods. We introduce isochrones of radio millisecond pulsars in the  $P\dot{P}$ -diagram to follow their spin evolution and discuss their true ages from comparison with observations. Finally, we apply our results of the spin-up process to complement our investigation of the massive pulsar PSR J1614–2230 from Paper I, confirming that this system formed via stable Case A RLO in an IMXB and enabling us to put new constraints on the birth masses of a number of recycled pulsars.

**Key words:** stars: neutron - white dwarfs - stars: rotation - X-rays: binaries - pulsars: general - pulsars: individual: PSR J1614–2230

## 1 INTRODUCTION

Binary millisecond pulsars (BMSPs) represent the advanced phase of stellar evolution in close, interacting binaries. Their observed orbital and stellar properties are fossil records of their evolutionary history. Thus one can use binary pulsar systems as key probes of stellar astrophysics. It is well established that the neutron star component in binary millisecond pulsar systems forms first, descending from the initially more massive of the two binary zero-

age main sequence (ZAMS) stars. The neutron star is subsequently spun up to a high spin frequency via accretion of mass and angular momentum once the secondary star evolves (Alpar et al. 1982; Radhakrishnan & Srinivasan 1982; Bhattacharya & van den Heuvel 1991). In this recycling phase the system is observable as a low-mass X-ray binary (e.g. Hayakawa 1985; Nagase 1989; Bildsten et al. 1997) and towards the end of this phase as an X-ray millisecond pulsar (Wijnands & van der Klis 1998; Archibald et al. 2009; Patruno & Watts 2012). Although this standard for-

mation scenario is commonly accepted many aspects of the mass-transfer process and the accretion physics are still not understood in detail (Lewin & van der Klis 2006). Examples of such ambiguities include the accretion disk structure, the disk-magnetosphere transition zone, the accretion efficiency, the decay of the surface B-field of the neutron star and the outcome of common envelope evolution.

The current literature on the recycling process of pulsars is based on a somewhat simplified treatment of both the accretion process and the so-called equilibrium spin theory, as well as the application of a pure vacuum magnetic dipole model for estimating the surface B-field strength of a radio pulsar. These simplifications become a problem when trying to probe the formation and the evolution of observed recycled radio pulsars located near the classical spin-up line for Eddington accretion in the  $P\dot{P}$ -diagram (e.g. Freire et al. 2011). In this paper we discuss the concept and the location of the spin-up line and investigate to which extent it depends on the assumed details of the accretion disk/magnetosphere interactions and the magnetic inclination angle of the pulsar. Furthermore, we include the plasma filled magnetosphere description by Spitkovsky (2006) for determining the surface B-field strengths of pulsars in application to spin-up theory and compare to the case of using the standard vacuum dipole model.

A key quantity to understand the formation of any given recycled radio pulsar is its spin period which is strongly related to the amount of mass accreted. The amount of accumulated mass is again determined by the mass-transfer timescale of the progenitor X-ray binary (and partly by the mode of the mass transfer and mass loss from the system), and hence it depends crucially on the nature of the donor star. At present the scenario is qualitatively well understood where low-mass X-ray binaries (LMXBs) and intermediate-mass X-ray binaries (IMXBs) in general lead to the formation of pulsars with a helium white dwarf (He WD) or a carbon-oxygen white dwarf (CO WD) companion, respectively (e.g. Tauris et al. 2000; Podsiadlowski et al. 2002; Deloye 2008; Tauris 2011). However, here we aim to quantify this picture in more detail by re-analysing the spin-up process. As an example, we investigate in this paper the possibilities of spinning up a neutron star from Case BB RLO leading to a mildly recycled pulsar with a CO WD companion. We also discuss the increasing number of systems which apparently do not fit the characteristics of these two main populations of binary pulsars.

We follow the pulsar spin evolution during the final phase of the mass transfer by including calculations of the torque acting on an accreting pulsar during the Roche-lobe decoupling phase (RLDP; Tauris 2012) for both an LMXB and an IMXB and compare the results. To complete the full history of pulsar spin evolution we subsequently consider the true ages of recycled radio pulsars (which are intimately related to their spin evolution) by calculating isochrones and discussing the distribution of recycled pulsars in the  $P\dot{P}$ -diagram.

Although accreting X-ray millisecond pulsars (AXMSPs) are believed to be progenitors of BMSPs, all of the 14 observed AXMSPs have orbital periods less than one day whereas fully recycled radio BMSPs are observed with orbital periods all the way up to a few hundred days (see also Tauris 2012). This puzzle will be inves-

tigated in a future paper. For the evolution of ultra-compact X-ray binaries (UCXBs) leading to AXMSPs, and later to the formation of tight-orbit recycled radio BMSPs with ultra-light ( $< 0.08 M_{\odot}$ ) companions, we refer to Podsiadlowski et al. (2002); Deloye & Bildsten (2003); van der Sluys et al. (2005); van Haaften et al. (2012). In this paper we focus on the formation and evolution of BMSPs with regular He WDs and CO/ONeMg WDs.

The discovery of PSR J1614–2230 (Hessels et al. 2005; Demorest et al. 2010) plays an important role for understanding BMSP formation. This pulsar system is interesting since it has a unique combination of a short pulsar spin period of 3.2 ms and a massive CO WD companion. A rapidly spinning pulsar is usually associated with a long phase of mass-transfer evolution in an LMXB, whereas a CO WD companion in a relatively close orbit (8.7 days) is evidently the outcome of an IMXB evolution. A possibly solution to this paradox is that PSR J1614–2230 evolved from Case A RLO of an IMXB which results in both a relatively long-lived X-ray phase ( $> 10^7$  yr), needed to spin up the pulsar effectively, and leaving behind a CO WD. In this case PSR J1614–2230 is the first BMSP known to have evolved via this path. Indeed, in Tauris et al. (2011), hereafter Paper I, we investigated the progenitor evolution of PSR J1614–2230 with emphasis on the X-ray phase where the binary contained a neutron star and a donor star. We found two viable possibilities for the formation of the PSR J1614–2230 system: either it contained a  $2.2 - 2.6 M_{\odot}$  asymptotic giant branch donor star and evolved through a common envelope and spiral-in phase initiated by Case C RLO, or it descended from a close binary system with a  $4.0 - 5.0 M_{\odot}$  main sequence donor star via Case A RLO as hinted above. The latter scenario was also found by Lin et al. (2011). The fact that PSR J1614–2230 was spun-up to (less than) 3.2 ms could indeed hint which one of the two formation scenarios is most likely. In order to test this idea and to further distinguish between Case A and Case C we turn our attention, here in Paper II, to the spin dynamics of this pulsar in the recycling process.

As discussed in Paper I, the distribution of neutron star birth masses is an important probe of both stellar evolution, binary interactions and explosion physics. For a number of BMSPs we are now able to put constraints on the birth mass of the pulsar given the derived amount of mass needed to spin up the observed recycled pulsar. In particular, it is of interest to see if we can identify further pulsars showing evidence of being born massive ( $\sim 1.7 M_{\odot}$ ) like PSR J1614–2230.

In order to understand the many different observational properties of BMSPs we have combined a variety of subtopics here with the aim of presenting a full picture of the subject. Given the many facets included, our new findings and the resulting length of the manuscript, we have chosen throughout this paper to finalize individual subtopics with a direct comparison to observational data followed by discussions in view of our theoretical modelling.

Our paper is structured in the follow way: We begin with a brief, updated review of the formation channels of BMSPs with CO WDs (Section 2) and present a summary of the latest observational data in Section 3. In this section we also demonstrate an emerging unified picture of pulsar formation history which, however, is challenged by a num-

ber of interesting systems which share expected properties of both an LMXB and an IMXB origin. In Section 4 we investigate the recycling process in general with a focus on the location of the spin-up line in the  $P\dot{P}$ -diagram and also relate the initial spin of a rejuvenated pulsar to the amount of mass accreted. The theoretical modelling is continued in Section 5 where we highlight the effects of the Roche-lobe decoupling phase on the spin evolution of recycled pulsars. In Section 6 our results are compared to the observed spin period distributions and in Section 7 we investigate if BMSPs with CO WD companions obtained their fast spin periods *after* a common envelope evolution. In Section 8 we discuss our results in a broader context in relation to the spin evolution and the true ages of millisecond radio pulsars. In Section 9 we continue our discussion from Paper I on the formation and evolution of PSR J1614–2230 and in Section 10 we return to the question of neutron star birth masses. Our conclusions are summarized in Section 11. Finally, in the Appendix we present a new tool to identify the most likely nature of the companion star to any observed binary pulsar.

## 2 FORMATION OF BMSPS WITH CO WD COMPANIONS

According to stellar evolution theory one should expect radio pulsars to exist in binaries with a variety of different companions: white dwarfs (He WDs, CO WDs and ONeMg WDs), neutron stars, black holes, ultra light semi-degenerate dwarfs (i.e. substellar companions or even planets), helium stars, main sequence stars and, for very wide systems, sub-giant and giant stars (Bhattacharya & van den Heuvel 1991; Tauris & van den Heuvel 2006, and references therein). Of these possibilities, pulsars orbiting black holes, helium stars and giant stars still remain to be detected.

The majority of radio BMSPs have He WD companions. The formation of these systems is mainly channeled through LMXBs and have been well investigated in previous studies (e.g. Webbink et al. 1983; Pylyser & Savonije 1988, 1989; Rappaport et al. 1995; Ergma et al. 1998; Tauris & Savonije 1999; Podsiadlowski et al. 2002; Nelson et al. 2004; van der Sluys et al. 2005; Deloye 2008). These systems have orbital periods between less than 0.2 days and up to several hundred days. One of the most striking features of these systems is the relation between white dwarf masses and orbital periods (e.g. Tauris & Savonije 1999). However, BMSPs with He WD companions may also form in IMXBs if Case A RLO is not initiated too late during the main sequence evolution of the donor star (Tauris et al. 2000; Podsiadlowski et al. 2002). In Section 3 we identify 6 BMSPs which may have formed via this channel.

BMSP systems with relatively heavy WDs (CO or ONeMg WDs) all have observed orbital periods  $\leq 40$  days. For these systems there are a number of suggested formation channels which are briefly summarized below – see Paper I, and references therein, for a more rigorous discussion. In order to leave behind a CO WD, its progenitor must be more massive than  $3.0 M_{\odot}$  if Roche-lobe overflow (RLO) is initiated while the donor star is still on the main sequence. If the

donor star is an asymptotic giant branch (AGB) star when initiating mass transfer it can, for example, have a mass as low as  $2.2 M_{\odot}$  and still leave behind a  $0.5 M_{\odot}$  CO WD remnant – see fig. 1 in Paper I. CO WDs in close binaries have masses between  $0.33\text{--}1.0 M_{\odot}$ , whereas the ONeMg WDs are slightly heavier with masses of  $1.1\text{--}1.3 M_{\odot}$ . The upper limit for the initial mass of donor stars in X-ray binaries leaving an ONeMg WD is often assumed to be about  $7\text{--}8 M_{\odot}$  (Podsiadlowski et al. 2004), depending on the orbital period, metallicity, treatment of convection and the amount of convective overshooting. However, Wellstein & Langer (1999) demonstrated that even stars with an initial mass in excess of  $13 M_{\odot}$  may form an ONeMg WD if these progenitor stars are in a tight binary and thus lose their envelope at an early stage via Case A RLO. Stars exceeding the upper threshold mass for producing an ONeMg WD will leave behind a neutron star remnant via an electron capture supernova (Nomoto 1984; Podsiadlowski et al. 2004) or via a core-collapse supernova of type Ib/c for slightly more massive stars. For single stars, or very wide binaries, the critical ZAMS mass for neutron star production via type II supernovae is about  $10 M_{\odot}$  (Zhang et al. 2008).

In this paper we consider all systems with either a CO or an ONeMg WD as *one* population, denoted by CO WDs unless specified otherwise, and all scenarios listed below apply to BMSPs with both types of massive white dwarf companions. However, the required progenitor star masses are, in general, somewhat larger for the ONeMg WDs compared to the CO WDs. Despite these minor differences, the bottom line is that in all cases IMXBs are the progenitor systems of BMSPs with massive white dwarf companions.

### 2.1 IMXBs with Case A RLO

BMSPs with CO WDs, which formed via Case A RLO in IMXBs, evolve from donor stars with masses  $3\text{--}5 M_{\odot}$  and orbital periods of a few days (Tauris et al. (2000); Podsiadlowski et al. (2002); Paper I). The final orbital periods of the BMSPs are  $5\text{--}20$  days. The mass-transfer phase consists of three parts: A1, A2 and AB. Phase A1 is thermal time-scale mass transfer and lasts for about 1 Myr. The majority of the donor envelope is transferred at a high rate exceeding  $10^{-5} M_{\odot} \text{ yr}^{-1}$ . However, the accretion onto the neutron star is limited by the Eddington luminosity, corresponding to an accretion rate of a few  $10^{-8} M_{\odot} \text{ yr}^{-1}$ , and thus the far majority of the transferred material (up to 99.9%) is ejected from the system. Phase A2 is driven by the nuclear burning of the residual hydrogen in the core. The resulting mass-transfer rate is very low ( $< 10^{-9} M_{\odot} \text{ yr}^{-1}$ ) and only a few  $10^{-2} M_{\odot}$  of material is transferred towards the accreting neutron star in a time-interval of  $20\text{--}50$  Myr. Phase AB is caused by expansion of the donor star while undergoing hydrogen shell burning. The mass-transfer rate is  $10^{-8}\text{--}10^{-7} M_{\odot} \text{ yr}^{-1}$  and lasts for  $\sim 10$  Myr. A few  $0.1 M_{\odot}$  is transferred towards the accreting neutron star – significantly more than in the previous two phases, A1 and A2. As we shall see later on, this phase is responsible for spinning up the neutron star to become a millisecond pulsar.

## 2.2 IMXBs with early Case B RLO

Wider orbit IMXB systems evolve from donor stars which are in the Hertzsprung gap at the onset of the RLO. The orbital periods at the onset of the Case B RLO are about 3–10 days and donor masses of  $2.5–5.0 M_{\odot}$  are needed to yield a CO WD remnant in a BMSP system (Tauris et al. 2000; Podsiadlowski et al. 2002). The final orbital periods of the BMSPs are about 3–50 days. The mass-transfer rate in the IMXB phase is highly super-Eddington ( $10^{-5} M_{\odot} \text{ yr}^{-1}$ ) and thus the far majority of the transferred material is ejected. However, a few  $10^{-2} M_{\odot}$  are transferred to the neutron star – enough to create a mildly ( $> 10$  ms) spun-up millisecond pulsar, see Section 4.

Binaries with either more massive donor stars ( $> 5 M_{\odot}$ ) or initial periods in excess of 10 days will undergo dynamically unstable RLO (see Paper I, and references therein) leading to a common envelope and spiral-in. The outcome of the inspiral is probably a merger for Case B RLO, since for these stars the (absolute) binding energy of the envelope is too large to allow for its ejection – except if accretion luminosity of the neutron star can be efficiently converted into kinetic energy of the envelope.

## 2.3 IMXBs with Case C RLO and a common envelope

Donor stars in systems with very wide orbits ( $P_{\text{orb}} \simeq 10^2 – 10^3$  days) prior to the mass-transfer phase develop a deep convective envelope as they become giant stars before filling their Roche-lobe. The response to mass loss for these stars is therefore expansion which causes the stars to overfill their Roche-lobe even more. To exacerbate this problem, binaries also shrink in size if mass transfer occurs from a donor star somewhat more massive than the accreting neutron star. This causes further overfilling of the donor star Roche-lobe resulting in enhanced mass loss etc. This situation is a vicious circle that leads to a dynamically unstable, runaway mass transfer and the formation of a common envelope (CE) followed by a spiral-in phase, e.g. Paczynski (1976), Iben & Livio (1993), Ivanova et al. (2012). Whereas donor stars which initiate RLO during hydrogen shell burning still have relatively tightly bound envelopes, these stars here which initiate RLO on the AGB have only weakly bound envelopes (Han et al. 1994; Dewi & Tauris 2000). Hence, these donor stars can survive the spiral-in phase of the neutron star without merging. To leave a CO WD remnant from such wide-orbit systems the ZAMS masses of the progenitor stars (the donor stars of the IMXBs) must be  $2.2 – 6 M_{\odot}$  (Paper I), depending on the assumed amount of convective core-overshooting in the stellar models.

## 2.4 BMSPs with a CO WD from LMXBs

In addition to the formation channels from IMXBs, pulsars with a CO WD companion can, in rare cases, be produced from late Case B RLO in an LMXB system – e.g. see Table A1 in Tauris & Savonije (1999). The outcome is an extremely wide-orbit pulsar system ( $P_{\text{orb}} > 1000$  days) with a  $0.47 – 0.67 M_{\odot}$  CO WD and a slowly spinning pulsar. The pulsar B0820+02 ( $P = 0.86$  sec,  $P_{\text{orb}} = 1232$  days) is an

example of a system which followed this formation channel (cf. Section 3.2). It is an interesting fact that CO WDs produced from donor stars in IMXBs can be less massive than CO WDs produced in such LMXBs. In low-mass stars ( $\leq 2.2 M_{\odot}$ ) helium is ignited in a flash under degenerate conditions and CO WDs produced from these stars in LMXBs have minimum masses of  $0.47 M_{\odot}$ , whereas in cores of intermediate-mass stars helium ignites non-degenerately and CO WDs from IMXBs can be made with masses down to  $0.33 M_{\odot}$  (Kippenhahn & Weigert 1990; Tauris et al. 2000; Podsiadlowski et al. 2002).

## 2.5 BMSPs with a CO WD from AIC?

Under certain circumstances it may be possible for an accreting O-Ne-Mg WD to reach the Chandrasekhar mass limit and thereby implode to form a neutron star – the so-called accretion-induced collapse, AIC (Miyaji et al. 1980; Nomoto 1984; Canal et al. 1990). A neutron star formed this way may leave behind a radio pulsar. The necessary conditions for a pulsar formed this way to further accrete from the companion star and leaving behind, for example a BMSP with a CO WD companion, is investigated in a separate paper (Tauris et al., in preparation). However, the recycling process, which is the main topic in this paper, remains the same.

## 3 OBSERVATIONAL CHARACTERISTICS OF BMSPS WITH CO WD COMPANIONS

Before looking into the details of recycling a pulsar in an X-ray binary, we first summarize the observational properties of the end products, the BMSPs. This is important for our subsequent discussions and understanding of the theoretical modelling which constitutes the core of our work. Furthermore, we shall investigate if and how the BMSPs with CO WD companions can be distinguished from the large population of BMSPs with He WD companions. For this purpose we make use of the  $P\dot{P}$ -diagram, the Corbet diagram and information of orbital eccentricities.

### 3.1 The $P\dot{P}$ -diagram

In order to understand the formation and evolution of recycled pulsars we have plotted in the  $P\dot{P}$ -diagram in Fig. 1 the distribution of 103 binary radio pulsars located in the Galactic disk. The various companion types are marked with different symbols (see also Table 1). The majority of the companion stars are helium white dwarfs (He WDs). However, there is also a significant population of the more massive CO and ONeMg WDs, as well as pulsars with another neutron star as companion. In some systems the companion is still a main sequence star. In other (very tight) systems the companion has evolved into a semi-degenerate substellar remnant ( $< 0.08 M_{\odot}$ ) – possibly aided by evaporation caused by the illumination from the pulsar following an ultra-compact LMXB phase (Podsiadlowski 1991; Deloye & Bildsten 2003; van der Sluis et al. 2005; Bailes et al. 2011; van Haften et al. 2012). Pulsar systems found in globular clusters are not useful as probes of stellar evolution and binary interactions since their

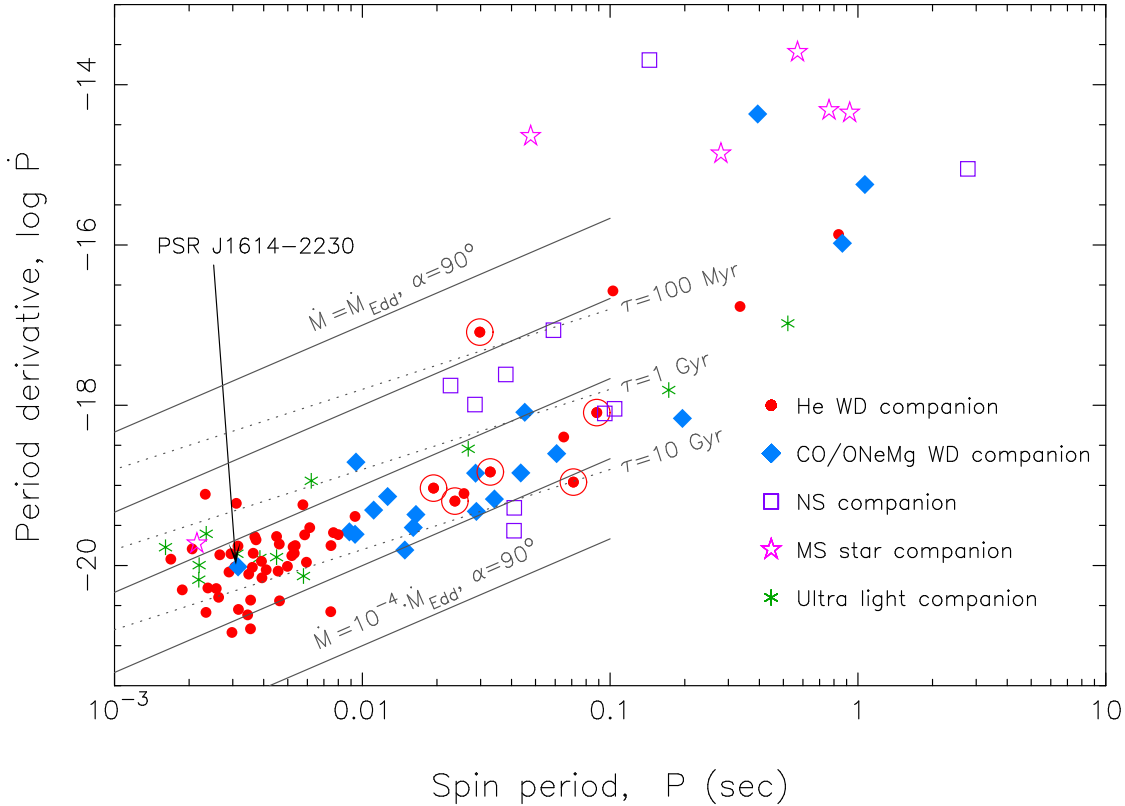


**Figure 1.** Distribution in the  $P\dot{P}$ -diagram of 103 binary radio pulsars in the Galactic disk. The five solid lines indicate theoretical spin-up lines using equation (10) for a  $1.4 M_{\odot}$  pulsar accreting with a rate of  $\dot{M} = \dot{M}_{\text{Edd}}$ ,  $0.1 \dot{M}_{\text{Edd}}$ ,  $0.01 \dot{M}_{\text{Edd}}$ ,  $0.001 \dot{M}$  and  $\dot{M} = 10^{-4} \dot{M}_{\text{Edd}}$ , respectively (top to bottom). Also shown as dotted lines are characteristic ages of 100 Myr, 1 Gyr and 10 Gyr, respectively. The location of PSR J1614–2230 is peculiar in the sense that it has a massive CO WD companion (blue diamond) in a region where all other pulsars have a low-mass He WD companion (red filled circles). The six pulsars marked with circles may have evolved from IMXBs and some of these are potential candidates for having a CO WD companion – see Section 3.2. Data taken from the *ATNF Pulsar Catalogue*, <http://www.atnf.csiro.au/research/pulsar/psrcat/> (Manchester et al. 2005), in May 2012.

location in a dense environment causes frequent exchange collisions whereby the orbital parameters are perturbed or the companion star is replaced with another star and thus information is lost regarding the mass transfer and spin-up of the pulsar. These pulsars could even have undergone accretion events from two or more different companions.

The location of PSR J1614–2230 in the  $P\dot{P}$ -diagram is quite unusual for a BMSP with a CO WD companion. It is located in an area which is otherwise only populated by BMSPs with He WD companions. This is important as it proves for the first time that efficient, full recycling (i.e.  $P \leq 8$  ms) of a pulsar is also possible in X-ray systems leading to BMSPs with CO WD companions. In general, the BMSPs with CO WD companions are seen to have large values of both  $P$  and  $\dot{P}$  compared to BMSPs with He WD companions. This trend can be understood since the former systems evolve from IMXBs which often have short lasting RLO and thus inefficient spin-up – PSR J1614–2230 being the only known exception (this system evolved from an IMXB via Case A RLO, see Paper I).

In Table 2 we list all binary radio pulsars with CO WD (or ONeMg WD) companions – see also Hobbs et al. (2004). At the bottom of the Table we list an additional number of sources which we identify as CO WD candidate systems (alternatively, these candidates may be He WDs evolving from

**Table 1.** Binary radio pulsars and their companions. Data taken from the *ATNF Pulsar Catalogue* in May 2012.

Population	Number
All known binary pulsars:	186
Galactic disk	110
Extra galactic (SMC)	1
Globular clusters	75
Galactic disk* binary pulsars with measured $\dot{P}$ :	103
Companion star:	
He white dwarf	56
CO/ONeMg white dwarf	19
Neutron star	10
Main sequence star*	6
Ultra light (semi)deg. dwarf, or planet(s)	12

\* Including PSR J0045–7319 which is located in the Small Magellanic Cloud and has a *B1V* companion (Kaspi et al. 1994).

IMXBs). The three slowest rotating of the 20 pulsars with a CO WD companion are not recycled – either because they were formed *after* the WD (Tauris & Sennels 2000), or be-

**Table 2.** Binary radio pulsars which are likely to have evolved from IMXB systems. Data taken from the *ATNF Pulsar Catalogue* in May 2012.

PSR	$P_{\text{orb}}$ days	$P$ ms	$\dot{P}$ $10^{-19}$	ecc $10^{-4}$	$M_{\text{WD}}$ $M_{\odot}$
J1952+2630	0.392	20.7	n/a	n/a	1.13
J1757-5322	0.453	8.87	0.263	0.0402	0.67
J1802-2124	0.699	12.6	0.726	0.0247	0.78*
B0655+64	1.03	196	6.85	0.0750	0.80
J1435-6100	1.35	9.35	0.245	0.105	1.08
J1439-5501	2.12	28.6	1.42	0.499	1.30*
J1528-3146	3.18	60.8	2.49	2.13	1.15
J1157-5112	3.51	43.6	1.43	4.02	1.30*
J1337-6423	4.79	9.42	1.95	0.197	0.95
J1603-7202	6.31	14.8	0.156	0.0928	0.34
J2145-0750	6.84	16.1	0.298	0.193	0.50
J1022+1001	7.81	16.5	0.433	0.970	0.85
J0621+1002	8.32	28.9	0.473	24.6	0.67*
J1614-2230	8.69	3.15	0.0962	0.0130	0.50*
J1454-5846	12.4	45.2	8.17	19.0	1.05
J0900-3144	18.7	11.1	0.491	0.0103	0.42
J1420-5625	40.3	34.1	0.675	35.0	0.44
J1141-6545 <sup>a</sup>	0.198	394	4307	1719	1.02*
B2303+46 <sup>a</sup>	12.3	1066	569	6584	1.30*
B0820+02 <sup>b</sup>	1232	865	105	118.7	> 0.52
J1622-6617 <sup>c</sup>	1.64	23.6	0.636	n/a	0.11
J1232-6501 <sup>c</sup>	1.86	88.3	8.11	1.09	0.17
J1745-0952 <sup>c</sup>	4.94	19.4	0.925	0.0985	0.13
J1841+0130 <sup>c</sup>	10.5	29.8	81.7	0.819	0.11
J1904+0412 <sup>c</sup>	14.9	71.1	1.10	2.20	0.26
J1810-2005 <sup>c</sup>	15.0	32.8	1.47	0.192	0.33

\* Mass obtained from timing. Other masses are median masses (i.e. calculated for  $i = 60^\circ$  and an assumed  $M_{\text{NS}} = 1.35 M_{\odot}$ ).

<sup>a</sup> A non-recycled pulsar formed *after* its WD companion (Tauris & Sennels 2000).

<sup>b</sup> This system descends from a very wide-orbit LMXB (see text).

<sup>c</sup> CO WD candidate or He WD evolving from an IMXB.

cause they formed in a very wide orbit (cf. Section 2.4). Of the remaining 17 recycled pulsars with a CO WD companion, 16 have a measured value of  $\dot{P}$ . These are plotted in Fig. 2 together with those other systems which may also have evolved from IMXB systems and thus possibly host a CO WD companion too (cf. Section 3.2). With the exception of PSR J1841+0130 (which is young, see Section 8.3.4), these pulsars are distributed in a somewhat more linear manner in the  $P\dot{P}$ -diagram compared to BMSPs with a He WD companion.

### 3.2 The Corbet diagram - six unusual pulsars

Plotting BMSPs in the Corbet diagram (Corbet 1984) could lead to potential clues about their formation history. In the top panel of Fig. 3 we have shown the distribution of all binary pulsars. Little can be learnt from this plot when considering the entire ensemble of binary pulsars as one population. In the central plot, however, we display only those binary pulsars which have a He WD companion. The distribution of pulsars in this diagram shows some interesting

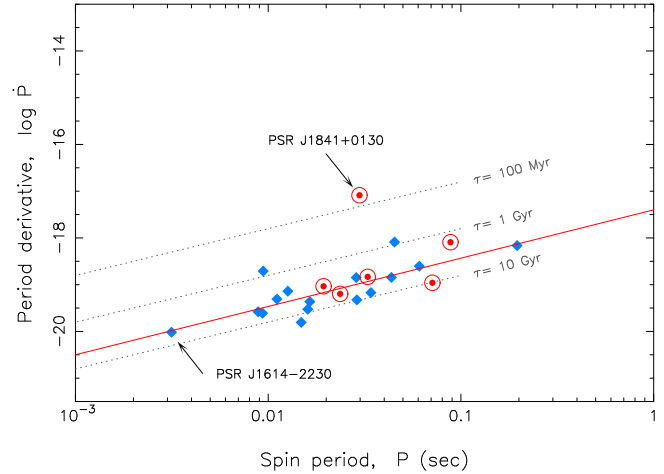


**Figure 2.** The observed recycled pulsars with CO WD companions (diamonds) seem to cluster somewhat along a straight line in the  $P\dot{P}$ -diagram. The full line is a linear regression fit to all these pulsars and the dotted lines represent constant characteristic ages. Other pulsars which are also candidates for having an IMXB origin are shown as dots in a circle (cf. Section 3.2). PSR J1841+0130 is a young example of such a candidate – see text.

features. The six pulsars marked with a circle are noticeable for having unusual slow spin periods compared to other pulsars with similar orbital periods, see Table 2 for further details. This fact hints an inefficient and shorter spin-up phase compared to the BMSPs with fast spin. Tauris (2011) suggested that these pulsars may perhaps have formed via the accretion induced collapse (AIC) of a WD. Here, we suggest instead that these pulsars (which all have  $P_{\text{orb}} \geq 1$  day) may have formed in IMXBs. In that case the companions are likely to be CO WDs, although He WD companions may also form from IMXBs (Tauris et al. 2000; Podsiadlowski et al. 2002). Similar ideas of an IMXB origin have been proposed by Camilo et al. (2001) and Li (2002). The latter author argued that accretion disk instabilities in IMXBs may explain the slow spin periods and the high  $\dot{P}$  values of these pulsars. The pulsars with  $P_{\text{orb}} > 200$  days all have slow spin periods – see Section 6.3 for a discussion on these systems. The bottom panel shows the binary pulsars with CO WD companions. The main thing to notice is that these systems have  $P_{\text{orb}} \leq 40^{\text{d}}$  and slower pulsar spin periods compared to BMSPs with He WD companions, as first pointed out by Camilo (1996). The slower spin of pulsars in this population can be understood well which is discussed further in Section 6. A few pulsars marked with a circle or a triangle stand out from the rest of the population. These are PSR J1141-6545 and PSR B2303+46 where the neutron star formed after the white dwarf companion (Tauris & Sennels 2000) and therefore these pulsars remain non-recycled with slow spin periods, and PSR B0820+02 which formed from an extremely wide-orbit LMXB with short lasting and possibly inefficient RLO (see Sections 2.4 and 6.3).

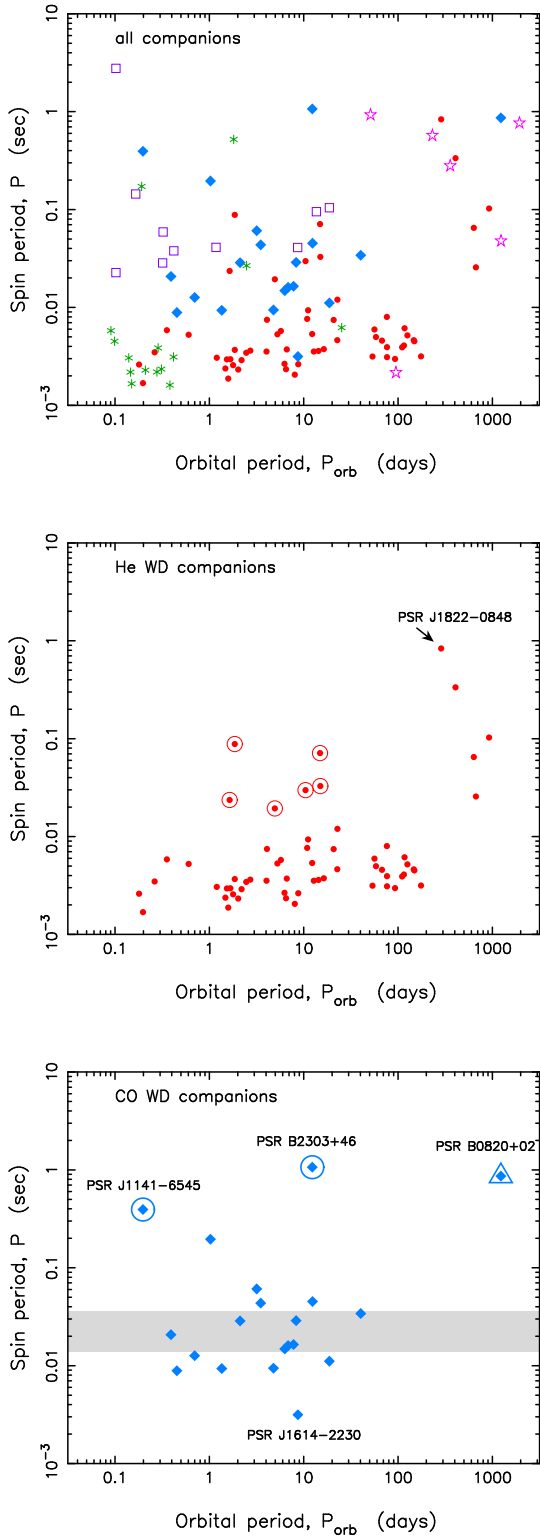


**Figure 3.** All binary radio pulsars in the Galactic disk plotted in a Corbet diagram (top), see Fig. 1 for an explanation of the symbols plotted. Due to their missing  $\dot{P}$  measurements 8 of these pulsars were not shown in Fig. 1. The central and bottom panels show the distribution of pulsars with He WD (60 systems) and CO WD companions (20 systems), respectively. In the bottom panel the grey shaded region marks the range of spin periods obtained from one of our model calculations of Case BB RLO in a post-CE binary (Fig. 10). See text for further discussion.

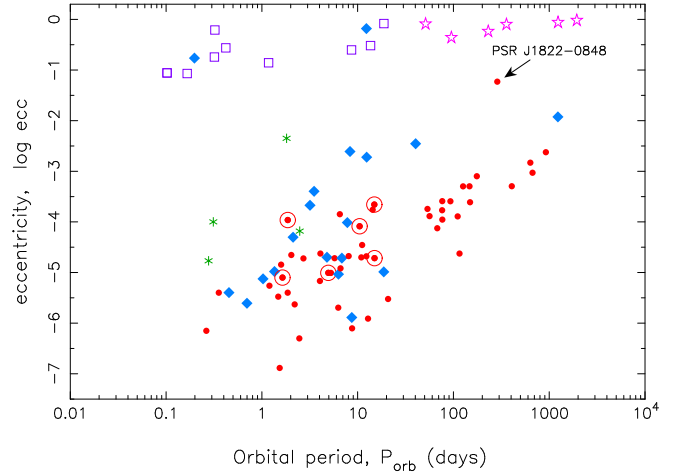


**Figure 4.** Eccentricity as a function of orbital period for binary radio pulsars in the Galactic disk. The various symbols are defined in Fig. 1. We notice PSR J1822–0848 which has an eccentricity two orders of magnitude larger than other wide-orbit binary pulsars with a He WD companion.

### 3.2.1 PSR J1841+0130

PSR J1841+0130 (discovered by Lorimer et al. 2006) is one of the six pulsars which we note to have an offset location in the Corbet diagram when comparing to BMSPs with He WD companions (Fig. 3, central panel). It has a slow spin period of 29 ms and an orbital period,  $P_{\text{orb}} = 10.5^{\text{d}}$ . The majority of other BMSPs with similar  $P_{\text{orb}}$  near 10 days have much faster spin periods between 2 – 10 ms. The slow spin period of PSR J1841+0130 can be explained if it originated from an IMXB system rather than an LMXB system. The mass function of this pulsar,  $f = 4.22 \times 10^{-4} M_{\odot}$  suggests that its companion star has a mass of  $0.11 M_{\odot}$  for an orbital inclination angle of  $60^{\circ}$ . If the companion star is a CO WD formed in an IMXB it must have a mass  $\geq 0.33 M_{\odot}$  (cf. Section 2.4). This would require a small inclination angle,  $i \leq 20^{\circ}$  (depending on the neutron star mass). The probability for this to happen from a distribution of random orbital orientations is about 6 per cent. The situation is similar in PSR J1622–6617 which is another candidate systems to have evolved from an IMXB. However, IMXBs can also leave behind He WDs which have somewhat smaller masses. Alternatively, if PSR J1841+0130 originated from an LMXB system then according to the  $(M_{\text{WD}}, P_{\text{orb}})$ -relation, e.g. Tauris & Savonije (1999), we would expect  $i \approx 25^{\circ}$  to obtain the predicted He WD mass of  $0.26 \pm 0.01 M_{\odot}$ . (The probability for this is about 9 per cent.) Hence, even in this case the inclination angle would be rather low. As discussed in Sections 4.3 and 8.3.4, PSR J1841+0130 is also interesting for its ability to constrain spin-up physics and for its young age.

### 3.3 The orbital eccentricity

Another fossil record of binary evolution is the orbital eccentricity (Phinney 1992; Phinney & Kulkarni 1994). In Fig. 4 we have plotted the eccentricity as a function of orbital period. The BMSPs with He WDs have in general somewhat

lower eccentricities than systems with CO WDs. The spread is large for both of the two populations which also overlap. Among the systems with CO WD companions it is not surprising that PSR J1614–2230 has the lowest eccentricity since we have demonstrated (Paper I) that this system formed via a relatively long phase of stable RLO. It is interesting to notice that the four BMSPs with CO WDs and  $P_{\text{orb}} < 2$  days all have quite small eccentricities  $\leq 10^{-5}$  even though they are believed to have formed via a CE.

### 3.3.1 PSR J1822–0848

PSR J1822–0848 (Lorimer et al. 2006) has an orbital period of 287 days and an eccentricity,  $ecc = 0.059$ . From Fig. 4 it is seen that this eccentricity is two orders of magnitude larger than that of other pulsars in similar wide-orbit systems. This fact, combined with its very slow spin period of 835 ms (see the central panel in Fig. 3) and its high value of  $\dot{P} = 1.35 \times 10^{-16}$ , hints that this pulsar may not have a He WD companion star. It is possible it belongs to the same class as PSR B0820+02 which is in a wide orbit with a CO WD (see Section 2.4). However, in that case it needs to be explained why some pulsars have He WD companions in even larger orbits compared to PSR J1822–0848. Alternatively, one could speculate that PSR J1822–0848 experienced weak spiral-in from an almost unbound common envelope of an AGB star. This could explain its non-recycled characteristics and why it has  $P_{\text{orb}} < 1000$  days.

Although, it has a relatively large eccentricity of 0.059 this value is still far too small to suggest that PSR J1822–0848 was born after the WD, like in the case of PSR 1141–6545 and PSR B2303+46 (Tauris & Sennels 2000). Even in the unrealistic case of a collapse of a naked core with no envelope, and without a kick, the present eccentricity of 0.059 for such a wide orbit would require a maximum instant mass loss of only  $\sim 0.10 M_{\odot}$  – a value which is even less than the release of the gravitational binding energy during the core collapse. Thus this scenario is not possible and we therefore conclude that PSR J1822–0848 was formed before its WD companion, like 99 per cent of all detected binary pulsars with WD companions.

## 4 RECYCLING THE PULSAR

We now proceed with a general examination of the recycling process of pulsars. We begin by analysing the concept of spin-up lines in the  $P\dot{P}$ -diagram and derive an analytic expression for the amount of accreted mass needed to spin up a pulsar to a given equilibrium spin period. We use standard theory for deriving these expressions, but include it here to present a coherent and detailed derivation needed for our purposes. Furthermore, we apply the Spitkovsky (2006) solution to the pulsar spin-down torque which combines the effect of a plasma current in the magnetosphere with the magnetic dipole model. The physics of the disk-magnetosphere interaction is still not known in detail. The interplay between the neutron star magnetic field and the conducting plasma in the accretion disk is a rather complex process. For further details of the accretion physics we refer to Pringle & Rees (1972); Lamb et al. (1973); Davidson & Ostriker (1973); Ghosh & Lamb

(1979a,b); Shapiro & Teukolsky (1983); Ghosh & Lamb (1992); Spruit & Taam (1993); Campana et al. (1998); Frank et al. (2002); Rappaport et al. (2004); Bozzo et al. (2009); D’Angelo & Spruit (2010); Ikhsanov & Beskrovnaya (2012) and references therein.

### 4.1 The accretion disk

The accreted gas from a binary companion possess large specific angular momentum. For this reason the flow of gas onto the neutron star is not spherical, but leads to the formation of an accretion disk where excess angular momentum is transported outwards by (turbulent-enhanced) viscous stresses, e.g. Shapiro & Teukolsky (1983); Frank et al. (2002). Depending on the mass-transfer rate, the opacity of the accreted material and the temperature of the disk, the geometric shape and flow of the material may take a variety of forms (thick disk, thin thick, slim disk, torus-like, ADAF). Popular models of the inner disk (Ghosh & Lamb 1992) include optically thin/thick disks which can be either gas (GPD) or radiation pressure dominated (RPD). The exact expression for the spin-up line in the  $P\dot{P}$ -diagram also depends on the assumed model for the inner disk – mainly as a result of the magnetosphere boundary which depends on the characteristics of the inner disk. Close to the neutron star surface the magnetic field is strong enough that the magnetic stresses truncate the Keplerian disk, and the plasma is channeled along field lines to accrete on to the surface of the neutron star. At the inner edge of the disk the magnetic field interacts directly with the disk material over some finite region. The physics of this transition zone from Keplerian disk to magnetospheric flow is important and determines the angular momentum exchange from the differential rotation between the disk and the neutron star. Interestingly enough, it seems to be the case that the resultant accretion torque, acting on the neutron star, calculated using detailed models of the disk-magnetosphere interaction does not deviate much from simple expressions assuming idealized, spherical accretion and newtonian dynamics. For example, it has been pointed out by Ghosh & Lamb (1992) as a fortuitous coincidence that the equilibrium spin period calculated under simple assumptions of spherical flow resembles the more detailed models of an optically thick, gas pressure dominated inner accretion disk. Hence, as a starting point this allows us to expand on standard prescriptions in the literature with the aims of: 1) performing a more careful analysis of the concept of a spin-up line, 2) deriving an analytic expression for the mass needed to spin up a given observed millisecond pulsar, and 3) understanding the effects on the spinning neutron star when the donor star decouples from its Roche-lobe. As we shall discuss further in Section 5, the latter issue depends on the location of the magnetospheric boundary (or the inner edge of the accretion disk) relative to the corotation radius and the light-cylinder radius of the pulsar. All stellar parameters listed below will refer to the neutron star unless explicitly stated otherwise.

### 4.2 The accretion torque – the basics

The mass transferred from the donor star carries with it angular momentum which eventually spins up the rotating neutron star once its surface magnetic flux density,  $B$  is low



enough to allow for efficient accretion, i.e. following initial phases where either the magneto-dipole radiation pressure dominates or propeller effects are at work.

The accretion torque acting on the spinning neutron star has a contribution from both material stress (dominant term), magnetic stress and viscous stress, and is given by:  $N = \dot{J}_\star \equiv (d/dt)(I\Omega_\star)$ , where  $J_\star$  is the pulsar spin angular momentum,  $\Omega_\star$  is its angular velocity and  $I \approx 1-2 \times 10^{45}$  g cm<sup>2</sup> is its moment of inertia. The exchange of angular momentum ( $\vec{J} = \vec{r} \times \vec{p}$ ) at the magnetospheric boundary eventually leads to a gain of neutron star spin angular momentum which can approximately be expressed as:

$$\Delta J_\star = \sqrt{GM} r_A \Delta M \xi \quad (1)$$

where  $\xi \simeq 1$  is a numerical factor which depends on the flow pattern (Ghosh & Lamb 1979b, 1992),  $\Delta M = \dot{M} \cdot \Delta t$  is the amount of mass accreted in a time interval  $\Delta t$  with average mass accretion rate  $\dot{M}$  and

$$\begin{aligned} r_A &\simeq \left( \frac{B^2 R^6}{\dot{M} \sqrt{2GM}} \right)^{2/7} \\ &\simeq 22 \text{ km } B_8^{4/7} \left( \frac{\dot{M}}{0.1 \dot{M}_{\text{Edd}}} \right)^{-2/7} \left( \frac{M}{1.4 M_\odot} \right)^{-5/7} \end{aligned} \quad (2)$$

is the Alfvén radius defined as the location where the magnetic energy density will begin to control the flow of matter (i.e. where the incoming material couples to the magnetic field lines and co-rotate with the neutron star magnetosphere). Here  $B$  is the surface magnetic flux density,  $R$  is the neutron star radius,  $M$  is the neutron star mass (see relation between  $R$  and  $M$  further below) and  $B_8$  is  $B$  in units of  $10^8$  Gauss. A typical value for the Alfvén radius in accreting X-ray millisecond pulsars (AXMSPs), obtained from  $B \sim 10^8$  G and  $\dot{M} \sim 0.01 \dot{M}_{\text{Edd}}$ , is  $\sim 40$  km corresponding to about  $3R$ . The expression above is found by equating the magnetic energy density ( $B^2/8\pi$ ) to the ram pressure of the incoming matter and using the continuity equation (e.g. Pringle & Rees 1972). Furthermore, it assumes a scaling with distance,  $r$  of the far-field strength of the dipole magnetic moment,  $\mu$  as:  $B(r) \propto \mu/r^3$  (i.e. disregarding poorly known effects such as magnetic screening (Vasyliunas 1979)). A more detailed estimation of the location of the inner edge of the disk, i.e. the coupling radius or magnetospheric boundary, is given by:  $r_{\text{mag}} = \phi \cdot r_A$ , where  $\phi$  is 0.5 – 1.4 (Ghosh & Lamb 1992; Wang 1997; D’Angelo & Spruit 2010).

#### 4.2.1 The surface B-field strength of recycled radio pulsars

Before we proceed we need an expression for  $B$ . One can estimate the B-field of recycled MSPs based on their observed spin period,  $P$  and its time derivative  $\dot{P}$ . The usual assumption is to apply the vacuum magnetic dipole model in which the rate of rotational energy loss ( $\dot{E}_{\text{rot}} = I\Omega\dot{\Omega}$ ) is equated to the energy-loss rate caused by emission of dipole waves (with a frequency equal to the spin frequency of the pulsar) due to an inclined axis of the magnetic dipole field with respect to the rotation axis of the pulsar:

$$\dot{E}_{\text{dipole}} = (-2/3c^3)|\ddot{\mu}|^2 \quad (3)$$

The result is:

$$\begin{aligned} B_{\text{dipole}} &= \sqrt{\frac{3c^3 I P \dot{P}}{8\pi^2 R^6}} \frac{1}{\sin \alpha} \\ &\simeq 1.6 \times 10^{19} \text{ G } \sqrt{P \dot{P}} \left( \frac{M}{1.4 M_\odot} \right)^{3/2} \frac{1}{\sin \alpha} \end{aligned} \quad (4)$$

where the magnetic inclination angle is  $0 < \alpha \leq 90^\circ$ . This is the standard equation for evaluating the B-field of a radio pulsar. Our numerical scaling constant differs by a factor of a few from the conventional one:  $B = 3.2 \times 10^{19} \text{ G } \sqrt{P \dot{P}}$ , which assumes  $R = 10$  km and  $I = 10^{45}$  g cm<sup>2</sup>, both of which we believe are slightly underestimated values (our assumed relations between  $I$ ,  $M$  and  $R$  are discussed in Section 4.2.2). Note also that some descriptions in the literature apply the polar B-field strength ( $B_p = 2B$ ) rather than the equatorial B-field strength used here.

It is important to realize that the above expression does not include the rotational energy loss obtained when considering the spin-down torque caused by the  $\vec{j} \times \vec{B}$  force exerted by the plasma current in the magnetosphere (e.g. Goldreich & Julian 1969; Spitkovsky 2008). For this reason the vacuum magnetic dipole model does not predict any spin-down torque for an aligned rotator ( $\alpha = 0^\circ$ ), which is not correct. The incompleteness of the vacuum magnetic dipole model was in particular evident after the discovery of intermittent pulsars by Kramer et al. (2006) and demonstrated the need for including the plasma term in the spin-down torque. A combined model was derived by Spitkovsky (2006) and applying his relation between  $B$  and  $\alpha$  we can rewrite the above expression slightly:

$$\begin{aligned} B &= \sqrt{\frac{c^3 I P \dot{P}}{4\pi^2 R^6}} \frac{1}{1 + \sin^2 \alpha} \\ &\simeq 1.3 \times 10^{19} \text{ G } \sqrt{P \dot{P}} \left( \frac{M}{1.4 M_\odot} \right)^{3/2} \sqrt{\frac{1}{1 + \sin^2 \alpha}} \end{aligned} \quad (5)$$

This new expression leads to smaller estimated values of  $B$  by a factor of at least  $\sqrt{3}$ , or more precisely  $\sqrt{\frac{3}{2}(2 + \cot^2 \alpha)}$ , compared to the vacuum dipole model. As we shall shortly demonstrate, this difference in dependence on  $\alpha$  is quite important for the location of the spin-up line in the  $P\dot{P}$ -diagram.

#### 4.2.2 The Eddington accretion limit

The Eddington accretion limit is given by:

$$\begin{aligned} \dot{M}_{\text{Edd}} &= \frac{4\pi c m_p}{\sigma_T} R \mu_e \\ &\simeq 3.0 \times 10^{-8} M_\odot \text{ yr}^{-1} R_{13} \left( \frac{1.3}{1+X} \right) \end{aligned} \quad (6)$$

where  $c$  is the speed of light in vacuum,  $m_p$  is the proton mass,  $\sigma_T$  is the Thomson scattering cross section,  $\mu_e = 2/(1+X)$  is the mean molecular weight per electron which depends on the hydrogen mass fraction,  $X$  of the accreted material, and  $R_{13}$  is the neutron star radius in units of 13 km. The expression is found by equating the outward radiation pressure to the gravitational force per unit area acting on the nucleons of the accreted plasma. In general, luminosity is generated from both nuclear burning at the neutron

star surface as well as from the release of gravitational binding energy of the accreted material, i.e.  $L = (\epsilon_{\text{nuc}} + \epsilon_{\text{acc}}) \dot{M}$ . However, for accreting neutron stars  $\epsilon_{\text{nuc}} \ll \epsilon_{\text{acc}}$  and thus we have neglected the contribution from nuclear processing. To estimate the neutron star radius we used a mass-radius exponent following a simple non-relativistic degenerate Fermi-gas polytrope ( $R \propto M^{-1/3}$ ) with a scaling factor such that:  $R = 15 (M/M_{\odot})^{-1/3}$  km, calibrated from PSR J1614–2230, cf. fig. 3 in Demorest et al. (2010). In our code the value of  $\dot{M}_{\text{Edd}}$  is calculated according to the chemical composition of the transferred material at any given time. Note, the value of  $\dot{M}_{\text{Edd}}$  is only a rough measure since the derivation assumes spherical symmetry, steady state accretion, Thompson scattering opacity and Newtonian gravity.

### 4.3 The spin-up line

The observed spin evolution of accreting neutron stars often shows rather stochastic variations on a short timescale (Bildsten et al. 1997). The reason for the involved dramatic torque reversals is not well known – see hypotheses listed at the beginning of Section 5. However, the long-term spin rate will eventually tend towards the *equilibrium* spin period,  $P_{\text{eq}}$  – meaning that the pulsar spins at the same rate as the particles forced to corotate with the  $B$ -field at the magnetospheric boundary. The location of the associated so-called spin-up line for the rejuvenated pulsar in the  $P\dot{P}$ -diagram can be found by considering the equilibrium configuration when the angular velocity of the neutron star is equal to the Keplerian angular velocity of matter at the magnetospheric boundary where the accreted matter enters the magnetosphere, i.e.  $\Omega_{\star} = \Omega_{\text{eq}} = \omega_c \Omega_{\text{K}}(r_{\text{mag}})$  or:

$$\begin{aligned} P_{\text{eq}} &= 2\pi \sqrt{\frac{r_{\text{mag}}^3}{GM}} \frac{1}{\omega_c} \\ &\simeq 1.40 \text{ ms} B_8^{6/7} \left( \frac{\dot{M}}{0.1 \dot{M}_{\text{Edd}}} \right)^{-3/7} \left( \frac{M}{1.4 M_{\odot}} \right)^{-5/7} R_{13}^{18/7} \end{aligned} \quad (7)$$

where  $0.25 < \omega_c \leq 1$  is the so-called critical fastness parameter which is a measure of when the accretion torque vanishes (depending on the dynamical importance of the pulsar spin rate and the magnetic pitch angle, Ghosh & Lamb 1979b). One must bear in mind that factors which may differ from unity were omitted in the numerical expression above. In all numerical expressions in this paper we assumed  $\sin \alpha = \phi = \xi = \omega_c = 1$ . Actually, the dependence on the neutron star radius,  $R$  disappears in the full analytic formula obtained by inserting equations (2) and (5) into the top expression in equation (7), and using  $r_{\text{mag}} = \phi \cdot r_{\Lambda}$ , which yields:

$$P_{\text{eq}} = \left( \frac{\pi c^9}{\sqrt{2} G^5 M^5 \dot{M}^3} \right)^{1/4} (1 + \sin^2 \alpha)^{-3/4} \phi^{21/8} \omega_c^{-7/4} \quad (8)$$

Notice, in the above step we needed to link the B-fields of accreting neutron stars to the B-fields (expressed by  $P$  and  $\dot{P}$ ) estimated for observed recycled radio pulsars. This connection can be approximated in the following manner: If the radio pulsar after the recycling phase is “born” with a spin period,  $P_0$  which is somewhat close to  $P_{\text{eq}}$  (i.e. if the Roche-lobe decoupling phase (RLDP) did not significantly affect the spin period of the pulsar, cf. discussion in Section 5), then we can estimate the location of its magnetosphere when

the source was an AXMSP just prior to the accretion turn-off during the RLDP. (Further details of our assumptions of the B-fields of accreting neutron stars are given in Section 4.4.1, and in Section 8 we discuss the subsequent spin evolution of recycled radio pulsars towards larger periods,  $P > P_0$ .)

It is often useful to express the time derivative of the spin period as a function the equilibrium spin period, for example for the purpose of drawing the spin-up line in the  $P\dot{P}$ -diagram:

$$\dot{P} = \frac{2^{1/6} G^{5/3} \dot{M} M^{5/3} P_{\text{eq}}^{4/3}}{\pi^{1/3} c^3 I} (1 + \sin^2 \alpha) \phi^{-7/2} \omega_c^{7/3} \quad (9)$$

Given that  $\dot{M}_{\text{Edd}}$  is a function of the neutron star radius and using the relation between  $M$  and  $R$  stated in Section 4.2.2 we need a relation between the moment of inertia and the mass of the neutron star. According to the equations-of-state studied by Worley et al. (2008) these quantities scale very close to linearly as:  $I_{45} \simeq M/M_{\odot}$  (see their fig. 4) where  $I_{45}$  is the moment of inertia in units of  $10^{45} \text{ g cm}^2$ . Towards the end of the mass-transfer phase the amount of hydrogen in the transferred matter is usually quite small ( $X \leq 0.20$ ). The donor star left behind is basically a naked helium core (the proto WD). Hence, we can use equation (6) and rewrite equation (9) to estimate the location of the spin-up line for a recycled pulsar in the  $P\dot{P}$ -diagram only as a function of its mass and its mass-accretion rate:

$$\dot{P} = 3.7 \times 10^{-19} (M/M_{\odot})^{2/3} P_{\text{ms}}^{4/3} \left( \frac{\dot{M}}{\dot{M}_{\text{Edd}}} \right) \quad (10)$$

assuming again  $\sin \alpha = \phi = \omega_c = 1$ , and where  $P_{\text{ms}}$  is the equilibrium spin period in units of milliseconds.

In the literature the spin-up line is almost always plotted without uncertainties. Furthermore, one should keep in mind the possible effects of the applied accretion disk model on the location of the spin-up line, cf. Section 4.1. In Fig. 5 we have plotted equation (9) for different values of  $\alpha$ ,  $\phi$  and  $\omega_c$  to illustrate the uncertainties in the applied accretion physics to locate the spin-up line. The upper boundary of each band (or “line”) is calculated for a neutron star mass  $M = 2.0 M_{\odot}$  and a magnetic inclination angle,  $\alpha = 90^\circ$ . The lower boundary is calculated for  $M = 1.0 M_{\odot}$  and  $\alpha = 0^\circ$ . The green hatched band corresponds to  $\phi = 1$  and  $\omega_c = 1$ , which we used in our calculations throughout this paper. The blue and red hatched bands are upper and lower limits set by reasonable choices of the two parameters ( $\phi$ ,  $\omega_c$ ). In all cases we assumed a fixed accretion rate of  $\dot{M} = \dot{M}_{\text{Edd}}$ . The location of the spin-up line is simply shifted one order of magnitude in  $\dot{P}$  down (up) for every order of magnitude  $\dot{M}$  is decreased (increased).

It is important to realize that there is no universal spin-up line in the  $P\dot{P}$ -diagram. Only an upper limit. Any individual pulsar has its own spin-up line/location which in particular depends on its unknown accretion history ( $\dot{M}$ ). Also notice that the dependence on the magnetic inclination angle,  $\alpha$  is much less pronounced when applying the Spitkovsky formalism for estimating the B-field of the MSP compared to applying the vacuum dipole model. The difference in the location of spin-up lines using  $\alpha = 90^\circ$  and  $\alpha = 0^\circ$  is only a factor of two in the Spitkovsky formalism. For a comparison, using the vacuum dipole model with a small magnetic inclination of  $\alpha = 10^\circ$  results in a spin-up

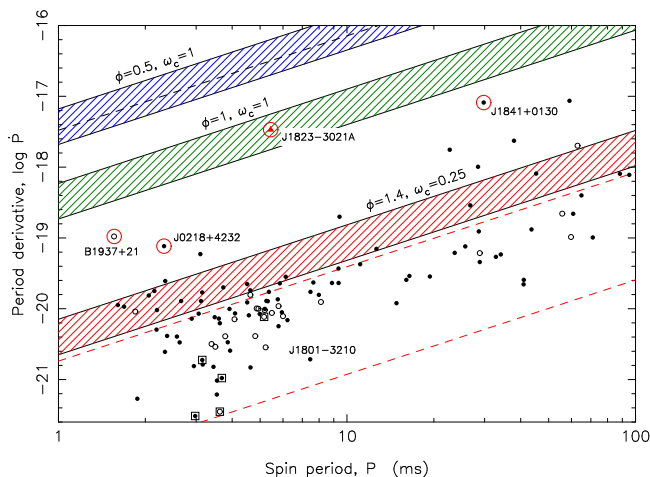


**Figure 5.** The spin-up line is shown as three coloured bands depending on the parameters ( $\phi$ ,  $\omega_c$ ). In all three cases the spin-up line is calculated assuming accretion at the Eddington limit,  $\dot{M} = \dot{M}_{\text{Edd}}$  and applying the Spitkovsky torque formalism. Thus these “lines” represent upper limits for the given set of parameters. The width of each line (band) results from using a spread in neutron star mass and magnetic inclination angle from ( $2.0 M_{\odot}$ ,  $\alpha = 90^{\circ}$ ) to ( $1.0 M_{\odot}$ ,  $\alpha = 0^{\circ}$ ), upper and lower boundary, respectively. The dashed line within the upper blue band is calculated from ( $2.0 M_{\odot}$ ,  $\alpha = 0^{\circ}$ ). Hence, the band width above this line reflects the dependence on  $\alpha$ , whereas the band width below this line shows the dependence on  $M$ . The two red dashed spin-up lines below the red band are calculated for a  $1.4 M_{\odot}$  neutron star using the vacuum magnetic dipole model for the radio pulsar torque and assuming  $\phi = 1.4$ ,  $\omega_c = 0.25$  and  $\dot{M} = \dot{M}_{\text{Edd}}$  for  $\alpha = 90^{\circ}$  (upper) and  $\alpha = 10^{\circ}$  (lower). The observed distribution of binary and isolated radio pulsars in the Galactic disk (i.e. outside globular clusters) are plotted as filled and open circles, respectively – see Fig. 13 for further information. Also plotted is the pulsar J1823–3021A which is located in the globular cluster NGC 6624. This pulsar and the three other pulsars marked by a red circle are discussed in the text.

line which is translated downwards by almost two orders of magnitude compared to its equivalent orthogonal rotator model, cf. the two red dashed lines in Fig. 5.

If we assume that accretion onto the neutron star is indeed Eddington limited then the three bands in Fig. 5 represent upper limits for the spin-up line for the given sets of ( $\phi$ ,  $\omega_c$ ). Thus we can in principle use this plot to constrain ( $\phi$ ,  $\omega_c$ ) and hence the physics of disk–magnetosphere interactions. The fully recycled pulsars B1937+21 and J0218+4232, and the mildly recycled pulsar PSR J1841+0130, are interesting since they are located somewhat in the vicinity of the green spin-up line. Any pulsar above the green line would imply that  $\phi < 1$ . The pulsar PSR J1823–3021A is close to this limit. Usually the derived value of  $\dot{P}$  for globular cluster pulsars is influenced by the cluster potential. However, the  $\dot{P}$  value for PSR J1823–3021A was recently constrained from Fermi LAT  $\gamma$ -ray observations (Freire et al. 2011) and for this reason we have included it here. The high  $\dot{P}$  values of the three Galactic field MSPs listed above: B1937+21, J0218+4232 and PSR J1841+0130, imply that these MSPs are quite young. We discuss their true ages in Sections 8.3.3 and 8.3.4.

#### 4.3.1 Formation of a submillisecond pulsar

The possible existence of submillisecond pulsars ( $P < 1$  ms) is a long standing and intriguing question in the literature since it is important for constraining the equation-of-state of neutron stars (e.g. Haensel & Zdunik 1989). There has been intense, but so far unsuccessful, efforts to detect these objects in either radio or X-rays (D’Amico 2000; Keith et al. 2010; Patruno 2010). We note from equation (7) that if the inner edge of the accretion disk (roughly given by  $r_{\text{mag}}$ ) extends all the way down to the surface of the neutron star we obtain the smallest possible value for  $P_{\text{eq}} \sim 0.6$  ms (depending on  $M$  and assuming  $\omega_c = 1$ ). It is possible to achieve  $r_{\text{mag}} \simeq R$  from a combination of a large value of  $\dot{M}$  and a small value of  $B$ , cf. equation (2).

#### 4.4 Amount of mass needed to spin up a pulsar

##### 4.4.1 Accretion-induced magnetic field decay

The widely accepted idea of accretion-induced magnetic field decay in neutron stars is based on observational evidence (e.g. Taam & van den Heuvel 1986; Shibazaki et al. 1989; Van Den Heuvel & Bitzaraki 1994). During the recycling process the surface B-field of pulsars is reduced by several orders of magnitude, from values of  $10^{11-12}$  G to  $10^{7-9}$  G. However, it is still not understood if this is caused by spin-down induced flux expulsion of the core proton fluxoids (Srinivasan et al. 1990), or if the B-field is confined to the crustal regions and decays due to diffusion and Ohmic dissipation, as a result of a decreased electrical conductivity when heating effects set in from nuclear burning of the accreted material (Geppert & Urpin 1994; Konar & Bhattacharya 1997), or if the field decay is simply caused by a diamagnetic screening by the accreted plasma – see review by Bhattacharya (2002) and references therein. Although there has been attempts to model or empirically fit the magnetic field evolution of accreting neutron stars (e.g. Shibazaki et al. 1989; Zhang & Kojima 2006; Wang et al. 2011) the results are quite uncertain. One reason is that it is difficult to estimate how much mass a given recycled pulsar has accreted. Furthermore, we cannot rule out the possibility that some of these neutron stars may originate from the accretion-induced collapse of a massive white dwarf, in which case they might be formed with a high B-field near the end of the mass-transfer phase.

To model the B-field evolution for our purpose, which is to relate the spin period of pulsars to the amount of mass accreted, we make the following assumptions:

- The B-field decays rapidly in the early phases of the accretion process via some unspecified process (see above).
- Accreting pulsars accumulate the majority of mass while spinning at/near equilibrium.
- The magnetospheric boundary,  $r_{\text{mag}}$  is approximately kept at a fixed location for the majority of the spin-up phase, until the mass transfer ceases during the RLDP, cf. Section 5.
- During the RLDP the B-field of an AXMSP can be considered to be constant since very little envelope material ( $\sim 0.01 M_{\odot}$ ) remains to be transferred from its donor at this stage.

4.4.2 *Accreted mass vs final spin period relation*

The amount of spin angular momentum added to an accreting pulsar is given by:

$$\Delta J_* = \int n(\omega, t) \dot{M}(t) \sqrt{GM(t)r_{\text{mag}}(t)} \xi(t) dt \quad (11)$$

where  $n(\omega)$  is a dimensionless torque, see Section 5 for a discussion. Assuming  $n(\omega) = 1$ , and  $M(t)$ ,  $r_{\text{mag}}(t)$  and  $\xi(t)$  to be roughly constant during the major part of the spin-up phase we can rewrite the expression and obtain a simple formula (see also equation 1) for the amount of matter needed to spin up the pulsar:

$$\Delta M \simeq \frac{2\pi I}{P\sqrt{GM}r_{\text{mag}}\xi} \quad (12)$$

Note, that the initial spin angular momentum of the pulsar prior to accretion is negligible given that  $\Omega_0 \ll \Omega_{\text{eq}}$ . To include all numerical scaling factors properly we can insert equations (2), (5) and (9) into equation (12), recalling that  $r_{\text{mag}} = \phi \cdot r_A$ , and we find:

$$\Delta M_{\text{eq}} = I \left( \frac{\Omega_{\text{eq}}^4}{G^2 M^2} \right)^{1/3} f(\alpha, \xi, \phi, \omega_c) \quad (13)$$

where  $f(\alpha, \xi, \phi, \omega_c)$  is some dimensionless number of order unity. Once again we can apply the relation between moment of inertia and mass of the neutron star (see Section 4.2.2) and we obtain a simple convenient expression to relate the amount of mass to be accreted in order to spin up a pulsar to a given (equilibrium) rotational period:

$$\Delta M_{\text{eq}} = 0.22 M_{\odot} \frac{(M/M_{\odot})^{1/3}}{P_{\text{ms}}^{4/3}} \quad (14)$$

assuming that the numerical factor  $f(\alpha, \xi, \phi, \omega_c) = 1$ .

In the above derivation we have neglected minor effects related to release of gravitational binding energy of the accreted material – see e.g. equation (22) in Tauris & Savonijje (1999), and in particular Bejger et al. (2011) and Bagchi (2011) for a more detailed, general discussion including various equations of state, general relativity and the critical mass shedding spin limit. However, since the exchange of angular momentum takes place near the magnetospheric boundary the expression in equation (14) refers to the baryonic mass accreted from the donor star. To calculate the increase in (gravitational) mass of the pulsar one must apply a reducing correction factor of  $\sim 0.85 - 0.90$ , depending on the neutron star equation-of-state (Lattimer & Yahil 1989).

In Fig. 6 we show the amount of mass,  $\Delta M_{\text{eq}}$  needed to spin up a pulsar to a given spin period. The value of  $\Delta M_{\text{eq}}$  is a strongly decreasing function of the pulsar spin period,  $P_{\text{eq}}$ . For example, considering a pulsar with a final mass of  $1.4 M_{\odot}$  and a recycled spin period of either 2 ms, 5 ms, 10 ms or 50 ms requires accretion of  $0.10 M_{\odot}$ ,  $0.03 M_{\odot}$ ,  $0.01 M_{\odot}$  or  $10^{-3} M_{\odot}$ , respectively. Therefore, it is no surprise that observed recycled pulsars with massive companions (CO WD, O-Ne-Mg WD or NS) in general are much more slow rotators – compared to BMSPs with He WD companions – since the progenitor of their massive companions evolved on a relatively short timescale, only allowing for very little mass to be accreted by the pulsar, cf. Section 6.

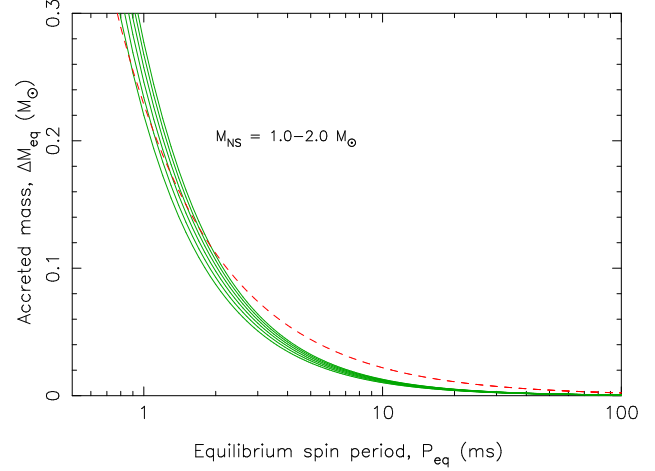


**Figure 6.** The amount of mass needed to spin up a pulsar as a function of its equilibrium spin period using equation (14). The different green curves correspond to various neutron star masses in steps of  $0.2 M_{\odot}$ , increasing upwards. The dashed red curve is the expression from equation (15) – see text.

4.4.3 *Comparison with other work*

The simple expression in equation (14) was also found by Alpar et al. (1982). Alternatively, one can integrate equation (12) directly which yields the maximum spin rate (minimum period) that can be attained by a neutron star accelerated from rest (Lipunov & Postnov 1984):

$$P_{\text{min}} = \frac{3\pi I}{\sqrt{G} r_{\text{mag}} \xi} \left( M^{3/2} - M_{\text{init}}^{3/2} \right)^{-1} \quad (15)$$

where  $M_{\text{init}} = M - \Delta M_{\text{eq}}$  is the mass of the neutron star prior to accretion. In this expression it is still assumed that  $I$  and  $r_{\text{mag}}$  remain constant during the accretion phase. For comparison, the expression above is also plotted in Fig. 6 as a dashed line assuming  $\Delta M_{\text{eq}} \ll M$ ,  $\xi = 1$  and  $r_{\text{mag}} = 22$  km (for example, if  $B = 10^8$  G,  $\dot{M} = 0.1 \dot{M}_{\text{Edd}}$ ,  $M = 1.4 M_{\odot}$ ,  $\phi = 1$ , see equation (2)). Although the latter expression is simplified with a chosen numerical value of  $r_{\text{mag}}$ , and the two expressions differ by more than a factor of two if  $P > 10$  ms, the overall match is fairly good.

On the one hand, the value of  $\Delta M_{\text{eq}}$  should be regarded as a lower limit to the actual amount of material required to be transferred to the neutron star, even at sub-Eddington rates, since a non-negligible amount may be ejected from the pulsar magnetosphere due to magnetodipole wave pressure or the propeller effect (Illarionov & Sunyaev 1975). Furthermore, accretion disk instabilities (Pringle 1981; van Paradijs 1996) are also responsible for ejecting part of the transferred material. Recently it was demonstrated by Antoniadis et al. (2012) that the accretion efficiency in some cases is less than 50 per cent, even in short orbital period binaries accreting at sub-Eddington levels. On the other hand, we did not take into account the possibility of a more efficient angular momentum transfer early in the accretion phase where the value of  $r_{\text{mag}}$  (the lever arm of the torque) could have been larger if the B-field did not decay rapidly. In this respect it is somewhat surprising that Wang et al. (2011), using a model for accretion induced B-field decay, find that it requires more

mass to be accreted to obtain a given spin period (see their fig. 6) compared to our work. This could perhaps (partly) be related to the fact that  $\Omega$  is small during the initial accretion phases.

#### 4.5 Spin-relaxation timescale

Above we have calculated the amount of mass needed to spin up a pulsar to a given equilibrium spin period. However, we must be sure that the accretion-torque can actually transmit this acceleration on a timescale shorter than the mass-transfer timescale. To estimate the spin-relaxation timescale (the time needed to spin up a slowly-rotating neutron star to spin equilibrium) one can simply consider:  $t_{\text{torque}} = J/N$  where  $J = 2\pi I/P_{\text{eq}}$  and  $N = \dot{M}\sqrt{GM r_{\text{mag}}}\xi$  which yields:

$$t_{\text{torque}} = I \left( \frac{4G^2 M^2}{B^8 R^{24} \dot{M}^3} \right)^{1/7} \frac{\omega_c}{\phi^2 \xi} \quad (16)$$

$$\simeq 50 \text{ Myr } B_8^{-8/7} \left( \frac{\dot{M}}{0.1 \dot{M}_{\text{Edd}}} \right)^{-3/7} \left( \frac{M}{1.4 M_{\odot}} \right)^{17/7}$$

or equivalently,  $t_{\text{torque}} = \Delta M/\dot{M}$ , see equation (12). If the duration of the mass-transfer phase,  $t_X$  is shorter than  $t_{\text{torque}}$  (this is the case if the mass-transfer rate  $|\dot{M}_2| \gg \dot{M}$ ) then the pulsar will not be fully recycled. In the following section we examine the importance of  $t_{\text{torque}}$  relative to the RLO turn-off timescale at the end of the mass-transfer process and how their ratio may affect the pulsar spin period.

### 5 ROCHE-LOBE DECOUPLING PHASE – RLDP

An important effect on the final spin evolution of accreting pulsars, related to the Roche-lobe decoupling phase (RLDP), has recently been demonstrated (Tauris 2012). The rapidly decreasing mass-transfer rate during the RLDP results in an expanding magnetosphere which may cause a significant braking torque to act on the spinning pulsar. It was shown that this effect can explain why the recycled radio MSPs (observed *after* the RLDP) are significantly slower rotators compared to the rapidly spinning accreting X-ray MSPs (observed *before* the RLDP). This difference in spin periods was first noted by Hessels (2008). However, only for MSPs with  $B > 10^8$  G can the difference in spin periods be partly understood from regular magnetodipole and plasma current spin-down of the recycled radio MSPs. In this section we investigate the RLDP effect on IMXBs and LMXBs and demonstrate different outcomes for BMSPs with CO and He WD companions. The purpose of the computations is to follow the spin evolution of the accreting X-ray millisecond pulsar (AXMSP) when the donor star decouples from its Roche-lobe, and to calculate the initial spin period of the recycled radio pulsar once the mass-transfer ceases. We model the main effect (the RLDP which causes the magnetosphere to expand dramatically) on the general spin evolution and ignore other, less known or somewhat hypothetical, dynamical effects during this epoch, such as warped disks, disk-magnetosphere instabilities, variations in the mass transfer rate caused by X-ray irradiation effects of the donor star, or transitions between a Keplerian thin disk and a sub-Keplerian, advection-

dominated accretion flow (ADAF) (e.g. Spruit & Taam 1993; Nelson et al. 1997; Yi et al. 1997; van Kerkwijk et al. 1998; Li & Wickramasinghe 1998; Locsei & Melatos 2004; Dai & Li 2006; Camero-Arranz et al. 2011, and references therein). Although many of these effects may be less important for the RLDP they could perhaps explain some of the frequent torque reversals observed in X-ray pulsars (Bildsten et al. 1997).

#### 5.1 Onset of a propeller phase

In the final stages of the X-ray phase, when the donor star is just about to detach from its Roche-lobe, the mass-transfer rate decreases significantly. This causes the ram pressure of the incoming flow to decrease whereby the magnetospheric boundary, and thus the coupling radius  $r_{\text{mag}}$ , moves outward. When this boundary moves further out than the corotation radius ( $r_{\text{mag}} > r_{\text{co}}$ ) given by:

$$r_{\text{co}} = \left( \frac{GM}{\Omega_*^2} \right)^{1/3} \quad (17)$$

$$\simeq 17 \text{ km } P_{\text{ms}}^{2/3} \left( \frac{M}{1.4 M_{\odot}} \right)^{1/3}$$

a centrifugal barrier arises since the plasma flowing towards the neutron star couples to the field lines in a super-Keplerian orbit. The material is therefore presumably ejected away from the neutron star in this propeller phase (Illarionov & Sunyaev 1975). This ejection of material causes exchange of angular momentum between the now relatively fast spinning neutron star and the slower spinning material at the edge of the inner disk. The result is a braking torque which acts to slow down the spin of the pulsar. This causes the corotation radius to move outwards too and the subsequent evolution is determined by the rate at which these two radii expand relative to one another. However, during the RLDP  $\dot{M}$  decreases too rapidly for  $r_{\text{co}}$  to keep up with the rapidly expanding  $r_{\text{mag}}$  and the equilibrium spin phase comes to an end.

In our model we assumed, in effect, that the inner edge of the accretion disk,  $r_{\text{disk}}$  follows  $r_{\text{mag}}$  and that the centrifugally expelled material has sufficient kinetic energy to be gravitationally unbound during the propeller phase when  $r_{\text{mag}} > r_{\text{co}}$ . These assumptions may not be entirely correct (Spruit & Taam 1993; Rappaport et al. 2004). For example, D’Angelo & Spruit (2010, 2011, 2012) recently demonstrated that accretion disks may be trapped near the corotation radius, even at low accretion rates. In this state the accretion can either continue to be steady or become cyclic. Furthermore, based on energy considerations they point out that most of the gas will not be ejected if the Keplerian corotation speed is less than the local escape speed. This will be the case if  $r_{\text{disk}} < 1.26 r_{\text{co}}$ . However, this trapped state only occurs in a narrow region around the corotation radius ( $\Delta r \ll r_{\text{co}}$ ) and given that  $r_{\text{mag}}/r_{\text{co}}$  often reaches a factor of 3–5 in our models at the end of the RLDP we find it convincing that the RLDP effect of braking the spin rates of the recycled pulsars is indeed present (see Tauris (2012) for further details).

### 5.1.1 The magnetosphere–disk interaction

In our numerical calculations of the propeller phase we included the effect of additional spin-down torques, acting on the neutron star, due to both magnetic field drag on the accretion disk (Rappaport et al. 2004) as well as magnetic dipole radiation (see equation (3)), although these effects are usually not dominant. It should be noted that the magnetic stress in the disk is also related to the critical fastness parameter,  $\omega_c$  (Ghosh & Lamb 1979b). We follow Tauris (2012) and write the total spin torque as:

$$N_{\text{total}} = n(\omega) \left( \dot{M} \sqrt{GM r_{\text{mag}}} \xi + \frac{\mu^2}{9r_{\text{mag}}^3} \right) - \frac{\dot{E}_{\text{dipole}}}{\Omega} \quad (18)$$

where

$$n(\omega) = \tanh \left( \frac{1 - \omega}{\delta_\omega} \right) \quad (19)$$

is a dimensionless function, depending on the fastness parameter,  $\omega = \Omega_\star / \Omega_K(r_{\text{mag}}) = (r_{\text{mag}}/r_{\text{co}})^{3/2}$ , which is introduced to model a gradual torque change in a transition zone near the magnetospheric boundary. The width of this zone has been shown to be small (Spruit & Taam 1993), corresponding to  $\delta_\omega \ll 1$  and a step-function-like behavior  $n(\omega) = \pm 1$ . In our calculations presented here we used  $\delta_\omega = 0.002$ ,  $\xi = 1$ ,  $r_{\text{disk}} = r_{\text{mag}}$  and also assumed the moment of inertia,  $I$ , to be constant during the RLDP. The latter is a good approximation since very little material is accreted during this terminal stage of the RLO.

### 5.1.2 Radio ejection phase

As the mass-transfer rate continues to decrease, the magnetospheric boundary eventually crosses the light-cylinder radius,  $r_{1c}$  of the neutron star given by:

$$r_{1c} = c/\Omega_\star \simeq 48 \text{ km } P_{\text{ms}} \quad (20)$$

When  $r_{\text{mag}} > r_{1c}$  the plasma wind of the pulsar can stream out along the open field lines, providing the necessary condition for the radio emission mechanism to turn on (e.g. Michel 1991; Spitkovsky 2008). Once the radio millisecond pulsar is activated the presence of the plasma wind may prevent further accretion from the now weak flow of material at low  $\dot{M}$  (Kluźniak et al. 1988). As discussed by Burderi et al. (2001, 2002) this will be the case when the total spin-down pressure of the pulsar (from magneto-dipole radiation and the plasma wind) exceeds the inward pressure of the material from the donor star, i.e. if:  $\dot{E}_{\text{rot}}/(4\pi r^2 c) > P_{\text{disk}}$ . However, it is interesting to notice that the recycled pulsar PSR J1023+0038 (Archibald et al. 2009) recently (within a decade) turned on its radio emission and it would indeed be quite a coincidence if we have been lucky enough to catch that moment – unless recycled pulsars evolve through a final phase with recurrent changes between accretion and radio emission modes.

## 5.2 Slow RLDP

In Fig. 7 we have shown a model calculation of the RLDP of an LMXB with an original donor star mass of  $1.1 M_\odot$ . The outcome was the formation of a BMSP with  $P = 5.2 \text{ ms}$  (assuming  $B = 1.0 \times 10^8 \text{ G}$ ) and a He WD companion of mass

$0.24 M_\odot$ , orbiting with a period of 5.0 days. It has been argued by Tauris & Savonije (1999); Antoniadis et al. (2012) that the majority of the transferred material in some LMXBs is lost from the system, even for accretion at sub-Eddington rates. Therefore, we assumed an effective accretion efficiency of 30 per cent in our LMXB model, i.e.  $\dot{M} = 0.30 |\dot{M}_2|$ , where  $|\dot{M}_2|$  is the RLO mass-transfer rate from the donor star. The accreted<sup>1</sup> mass-transfer rate  $\dot{M}$  is shown in the upper left panel.

The three phases: *equilibrium spin* (corresponding to  $r_{\text{mag}} \simeq r_{\text{co}}$ ), *propeller phase* ( $r_{\text{co}} < r_{\text{mag}} < r_{1c}$ ) and *radio pulsar* ( $r_{\text{mag}} > r_{1c}$ ) are clearly identified in this figure. During the equilibrium spin phase the rapidly alternating sign changes of the torque (partly unresolved on the graph in the lower left panel) reflect small oscillations around the semi-stable equilibrium, corresponding to successive small episodes of spin up and spin down. The reason is that the relative location of  $r_{\text{mag}}$  and  $r_{\text{co}}$  depends on the small fluctuations in  $\dot{M}$ . Despite applying an implicit coupling scheme in the code and ensuring that our time steps during the RLDP (about  $8 \times 10^4 \text{ yr}$ ) are much smaller than the duration of the RLDP ( $\sim 10^8 \text{ yr}$ ), our calculated mass-transfer rates are subject to minor numerical oscillations. However, these oscillations could in principle be physical within the frame of our simple model. Examples of physical perturbations that could cause real fluctuations in  $\dot{M}$ , but on a much shorter timescale, are accretion disk instabilities and clumps in the transferred material from the donor star (our donor stars have active, convective envelopes during the RLDP).

At some point the equilibrium spin is broken. Initially, the spin can remain in equilibrium by adapting to the decreasing value of  $\dot{M}$ . However, further into the RLDP the result is that  $r_{\text{mag}}$  increases on a timescale faster than the spin-relaxation timescale,  $t_{\text{torque}}$  at which the torque can transmit the effect of deceleration to the neutron star, and therefore  $r_{\text{mag}} > r_{\text{co}}$  (see Tauris 2012, and supporting online material therein). During the propeller phase the resultant accretion torque acting on the neutron star is negative, i.e. a spin-down torque. When the radio pulsar is activated and the accretion has come to an end, the spin-down torque is simply caused by the magneto-dipole radiation combined with the pulsar wind (see Section 4.2.1).

The aim here is to calculate the initial spin period of the recycled radio pulsar,  $P_0$  once the mass-transfer ceases. In this LMXB model calculation the value of the spin period increased significantly during the RLDP. The reason for this is that the duration of the propeller phase (i.e. the RLDP) is a substantial fraction of the spin-relaxation timescale,  $t_{\text{torque}}$ . Using equation (16) we find  $t_{\text{torque}} = 195 \text{ Myr}$  whereas the RLDP lasts for  $t_{\text{RLDP}} \simeq 56 \text{ Myr}$  which is a significant fraction of  $t_{\text{torque}}$  ( $t_{\text{RLDP}}/t_{\text{torque}} = 0.29$ ). Therefore, the RLDP has quite a significant impact on the spin evolution of the neutron star. It is seen that the spin period increases from 3.7 ms to 5.2 ms during this short time interval, i.e. the pulsar loses 50 per cent of its rotational energy during the RLDP. As shown by Tauris (2012) this RLDP effect is important for understanding the apparent difference in spin

<sup>1</sup> Strictly speaking this is the estimated mass-transfer rate received from the inner edge of the accretion disk. Some of this material is ejected during the propeller phase.

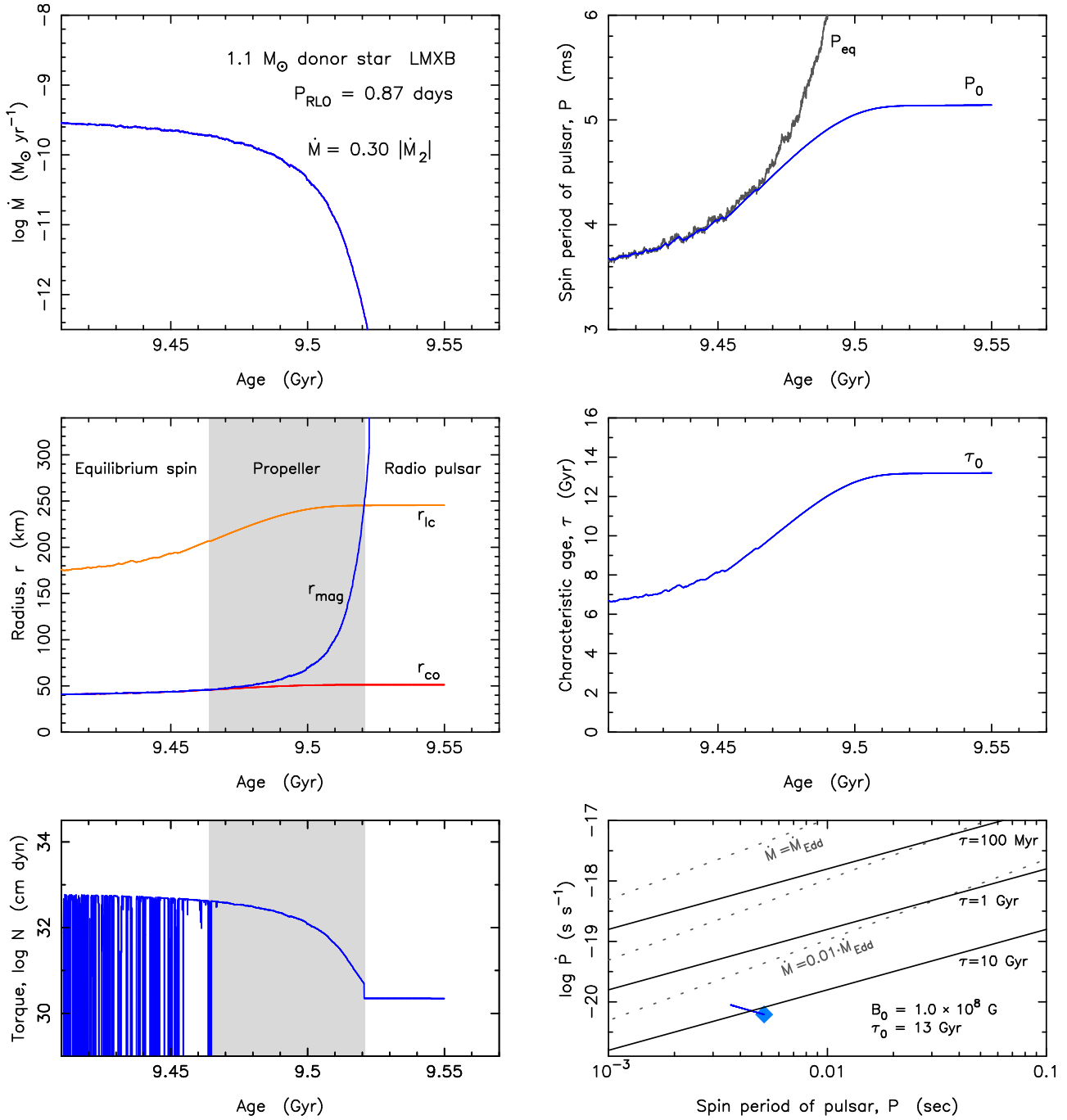


**Figure 7.** Example of a slow Roche-lobe decoupling phase (RLDP) and the final spin evolution of a pulsar formed with a He WD companion in an LMXB. The left side panels show: The accretion rate of the pulsar,  $\dot{M}$  as a function of the total age of the donor star (top); the evolution of the location of the magnetospheric boundary,  $r_{\text{mag}}$ , the corotation radius,  $r_{\text{co}}$  and the light-cylinder radius,  $r_{\text{ic}}$  (centre); and the resulting braking torque (bottom). The right side panels show: The evolution of the pulsar spin period as a function of the total age of the donor star (top); the evolution of the pseudo characteristic age of the pulsar (centre); and the RLDP evolutionary track leading to the birth location in the  $P\dot{P}$ -diagram shown as a blue diamond (bottom). The three epochs of the RLDP: *equilibrium spin*, *propeller phase* and *radio pulsar* are easily identified in the left side panels. The propeller phase is grey shaded. In these model calculations we assumed  $\sin \alpha = \phi = \xi = \omega_c = 1$  and  $\delta_\omega = 0.002$ . It is interesting to notice how the changes in the accretion rate,  $\dot{M}$  affects the magnetospheric coupling radius,  $r_{\text{mag}}$  which again affects the spin-down torque and the equilibrium spin period, cf. equations (2), (1) and (7). The reason why the spin of the pulsar (blue line, upper right panel) decouples from its equilibrium spin (black line) is that the spin-down torque cannot transmit the deceleration on a timescale short enough for the pulsar to adapt to its new equilibrium. In this example, the duration of the RLDP is a significant fraction of the spin-relaxation timescale of the accreting neutron star and thus the RLDP has a momentous impact on the rotational evolution. The birth spin period,  $P_0$  of this recycled pulsar is seen to deviate substantially from its original  $P_{\text{eq}}$  calculated at the onset of the RLDP. Furthermore, the effect on the characteristic age for this BMSP is also quite significant. During the 56 Myr of the RLDP it doubles to become  $\tau = 13$  Gyr at *birth*. Hence, many MSPs which appear to be old according to their  $\tau$  may in fact be quite young. See text for further discussions.

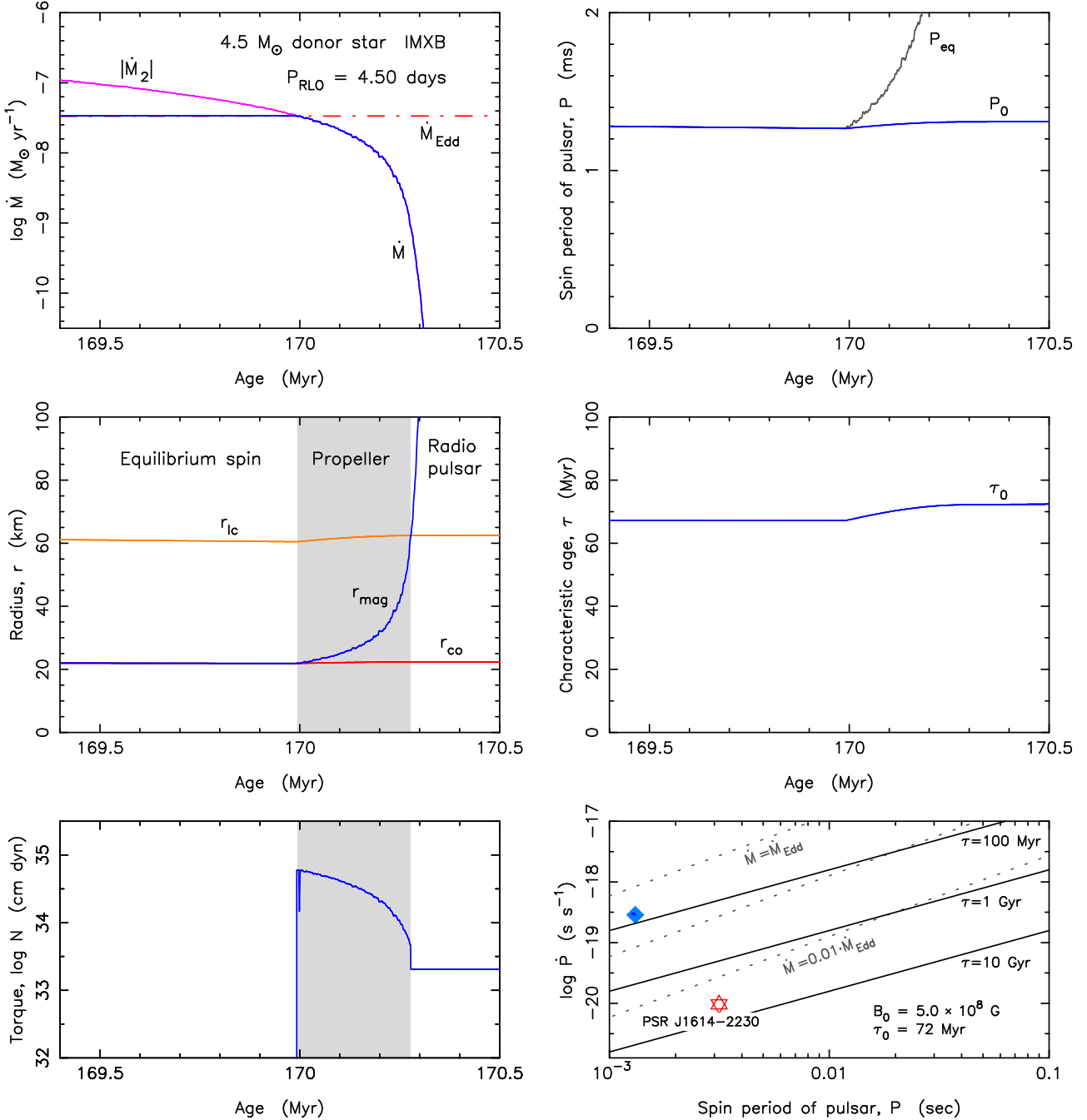


**Figure 8.** Example of a rapid Roche-lobe decoupling phase (RLDP) in an IMXB using our mass-transfer progenitor model of PSR J1614–2230. The spin evolution of the pulsar is shown during the RLDP when the IMXB donor star terminated its mass transfer. For a description of the various panels and their labels, see Fig. 7. In the  $P\dot{P}$ -diagram in the lower right panel the birth location, immediately following the RLDP, of the recycled radio pulsar is shown as a blue diamond for  $\sin \alpha = \phi = \xi = \omega_c = 1$ . The red star indicates the presently observed location of PSR J1614–2230. In Section 9.1 we argue that PSR J1614–2230 is more likely to have evolved with  $\sin \alpha < 1$ ,  $\phi > 1$  and  $\omega_c < 1$  which results in a birth location much closer to its present location in the  $P\dot{P}$ -diagram. In IMXBs where the donor star evolves on a relatively short timescale, the RLDP is rapid. Therefore, the spin evolution of the accreting X-ray pulsar (see blue line in upper right panel) freezes up near the original value of  $P_{\text{eq}}$ , i.e. the recycled radio pulsar is born with a spin period,  $P_0$  which is close to the equilibrium spin period of the accreting X-ray pulsar calculated at the time when the donor star begins to decouple from its Roche-lobe. In this IMXB model the mass-transfer rate,  $\dot{M} > \dot{M}_{\text{Edd}}$  and the accretion onto the neutron star is therefore limited by the Eddington mass-accretion rate (red dot-dashed line in the upper left panel). This explains the why the spin of the pulsar,  $P = P_{\text{eq}} \approx \text{const.}$  (top right panel) until  $\dot{M} < \dot{M}_{\text{Edd}}$ , as opposed to the situation in Fig. 7.



period distributions between AXMSPs<sup>2</sup> and radio MSPs (Hessels 2008). The black line labelled “ $P_{\text{eq}}$ ” in the upper right panel reflects the evolution of  $P$  in case the neutron star was able to instantly re-adjust itself to the changing  $P_{\text{eq}}$  (equation 7) during the RLDP. However, the neutron star possesses a large amount of rotational inertia and such rapid changes in  $P$  are not possible to transmit to the neutron star given the limited torque acting on it. Therefore the spin evolution terminates at the end of the blue line labelled “ $P_0$ ”. The small fluctuations of  $P_{\text{eq}}$  during the equilibrium spin phase reflect fluctuations in  $\dot{M}(t)$ .

The RLDP effect also causes a large impact on the characteristic age,  $\tau_0$ , of the radio pulsar at birth. In the central right panel we show how  $\tau_0$  doubles in value from 6.7 Gyr to 13 Gyr during the RLDP (see also the solid line ending at the blue diamond in the  $P\dot{P}$ -diagram in the lower right panel). The characteristic age at birth is given by:  $\tau_0 \equiv P_0/2\dot{P}_0$ , where  $\dot{P}_0$  can be estimated from the assumed B-field of the pulsar at this epoch. Actually, the “characteristic age” of the pulsar during the RLDP (which is plotted in the central right panel) is a pseudo age which is only relevant at the end point ( $\tau_0$ ) when the accretion has stopped. In order to construct the track leading to  $\tau_0$  we assumed  $B^2 \propto P\dot{P} = \text{const.}$  from equation (4), leading to  $\tau \propto P^2$ . During the RLDP it is a good approximation to assume a (final) constant value of the neutron star surface magnetic flux density,  $B$  since 99 per cent of the accretion onto the neutron star occurs before the final termination stage of the RLDP. In this case we assumed a final B-field strength of  $B = 1 \times 10^8$  G – a typical value for BMSPs with He WD companions. This example clearly reflects why characteristic ages of MSPs are untrustworthy as true age indicators since here the MSP is born with  $\tau_0 \simeq 13$  Gyr (see also Tauris (2012)). This fact is important since the characteristic ages of recycled pulsars are often compared to the cooling ages of their white dwarf companions (e.g. see discussion in van Kerkwijk et al. 2005).

### 5.3 Rapid RLDP ( $P_{\text{eq}}$ freeze-up)

In Fig. 8 we have plotted the RLDP during the final stages of the IMXB phase AB using our Case A model calculation of PSR J1614–2230 presented in Paper I. The initial conditions were a  $4.5 M_{\odot}$  donor star in an IMXB with an orbital period of 2.20 days. The final system was a BMSP with a  $0.50 M_{\odot}$  CO WD orbiting a  $1.99 M_{\odot}$  recycled pulsar with an orbital period of 8.7 days – resembling the characteristics of the PSR J1614–2230 system. The accretion rate onto the neutron star,  $\dot{M}$  (see blue line in upper left panel) is Eddington limited (red dot-dashed line) and hence  $\dot{M} = \min(|\dot{M}_2|, \dot{M}_{\text{Edd}})$  where  $|\dot{M}_2|$  represents the mass-transfer rate from the donor star (purple line). When the age of the donor star is  $\sim 170.0$  Myr the mass-transfer rate

becomes sub-Eddington and  $\dot{M}$  decreases with  $|\dot{M}_2|$ . From this point onwards  $r_{\text{mag}}$  increases as expected, as a result of the decreasing ram pressure, and it increases at a rate where  $r_{\text{co}}$  cannot keep up with it (see central panel, left column) and therefore the pulsar enters the propeller phase. After less than 0.3 Myr the accretion phase, and thus the propeller phase, is terminated when  $r_{\text{mag}} > r_{\text{lc}}$  and the radio ejection mechanism is activated.

During the equilibrium spin phase the net accretion torque acting on the pulsar is close to zero. This is not only due to our transition zone approximation (equation (19)) where the torque vanishes when  $r_{\text{mag}} \simeq r_{\text{co}}$ . If the transition zone was arbitrary thin ( $\delta_{\omega} \ll 1$ ), and  $n(\omega)$  would be a step-like function going from +1 to –1 (i.e. switch mode), there would be rapidly alternating sign changes of the torque during the equilibrium spin phase. Whereas small fluctuations in  $\dot{M}$  would lead to such rapid torque oscillations for sub-Eddington accretion (as seen in Fig. 7) the sharply defined Eddington limit applied here prevents such fluctuations during the equilibrium spin phase. However, the time-averaged torque would be close to zero in any case.

In this IMXB model calculation the value of the spin period only increased very little during the RLDP. The reason for this is that the duration of the RLDP ( $t_{\text{RLDP}} \simeq 0.28$  Myr) is relatively short compared to the spin-relaxation timescale ( $t_{\text{torque}} = 6.8$  Myr). The small ratio  $t_{\text{RLDP}}/t_{\text{torque}} \simeq 0.04$  at the onset of the RLDP causes the spin period to “freeze” at the original value of  $P_{\text{eq}}$  (see also Ruderman et al. 1989). Note, the values quoted above as well as rough values of  $t_{\text{torque}} = (2\pi/P)I/N$  and  $r_{\text{mag}} \simeq r_{\text{co}} \simeq 22$  km can be checked by reading numbers from the plots and using equations (2) and (17). The relevant numbers are:  $B = 5 \times 10^8$  G (a typical value for BMSPs with CO WD companions),  $\dot{M} \simeq \dot{M}_{\text{Edd}}$ ,  $M \simeq 1.99 M_{\odot}$ ,  $P_{\text{eq}} = 1.28$  ms and  $\log N = 34.8$ . For the spin-up process discussed here we assumed again  $\sin \alpha = \phi = \xi = \omega_c = 1$ .

#### 5.3.1 Rapid RLDP with a helium star donor

As discussed in Section 7 (and seen in Fig. 10) helium donor stars evolve on a short nuclear timescale compared to a normal hydrogen-rich donor. This leads to a rapid accretion turn-off lasting only a few  $10^4$  yr and therefore  $t_{\text{RLDP}}/t_{\text{torque}} \ll 1$ , which also in these systems causes  $P_0$  to “freeze” at the original value of  $P_{\text{eq}}$ .

### 5.4 RLDP in IMXB vs LMXB systems

The major difference between the RLDP in an IMXB (often leading to a BMSP with a CO WD) and the RLDP in an LMXB (leading to a BMSP with a He WD) is the time duration of the RLDP relative to the spin-relaxation timescale, i.e. the  $t_{\text{RLDP}}/t_{\text{torque}}$ -ratio. The mass-transfer in X-ray binaries proceeds much faster in IMXBs compared to LMXBs. Hence, also the termination of the RLDP is shorter in IMXBs, and therefore the  $t_{\text{RLDP}}/t_{\text{torque}}$ -ratio is smaller, compared to LMXBs. The conclusion is that, in general, we expect a significant RLDP effect only in LMXBs. (It may be possible, however, that the RLDP effect could play a more significant role in some IMXB systems if they leave behind a neutron star with a relatively high B-field, thereby decreasing  $t_{\text{torque}}$ ).

<sup>2</sup> The majority of the AXMSPs have very small  $P_{\text{orb}}$  (typically 1–2 hours) and substellar companions ( $< 0.08 M_{\odot}$ ) and hence most of these AXMSPs are not true progenitors of the general population of radio MSPs. However, the important thing is that the pulsars are spun up to rotational periods which seem to be almost independent of orbital period up to 200 days, as seen in the central panel of Fig. 3.

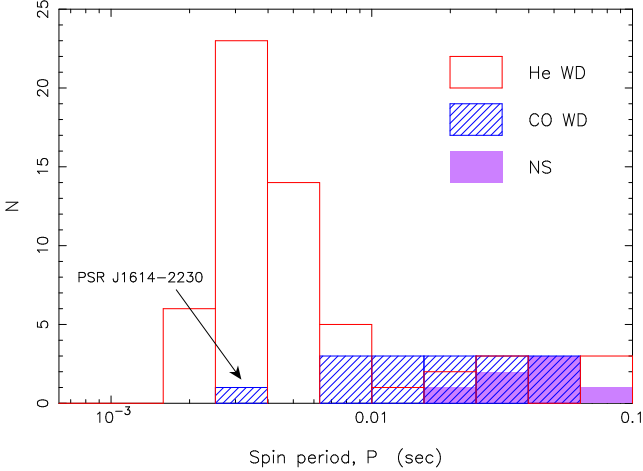


**Figure 9.** The observed spin period distribution of recycled pulsars in the Galactic disk with  $P < 100$  ms for pulsars with He WD and CO WD companions. The median spin periods for these populations are 3.9 ms and 16 ms, respectively. For comparison we have also shown the spin distribution of those recycled pulsars with neutron star companions and  $P < 100$  ms.

## 6 OBSERVED SPIN-PERIOD DISTRIBUTIONS

We now investigate if the empirical pulsar spin data can be understood in view of the theoretical modelling presented in the last couple of sections.

### 6.1 Recycled pulsars with WD companions

In Fig. 9 we have plotted histograms of the observed spin period distribution of recycled pulsars with He WD and CO WD companions. There are 57 known recycled pulsars in the Galactic disk with a He WD companion and a spin period  $P < 100$  ms (with or without a measured  $\dot{P}$ ) and these pulsars have a median spin period of 3.9 ms (the average spin period is 10 ms). The median spin period of the 16 known recycled pulsars with a CO WD companion and  $P < 100$  ms, however, is 16 ms (the average value is 23 ms). All observed BMSPs have lost rotational energy due to magneto-dipole radiation and a pulsar wind since they appeared as recycled pulsars. Hence, their current spin period,  $P$  is larger than their  $P_{\text{eq}}$ . Unfortunately, we have no empirical constraints on the spin-down torque acting on recycled radio MSPs and therefore their braking index remains unknown, cf. Section 8. Furthermore, in Section 5 we demonstrated that BMSPs formed in LMXBs lose rotational energy during the RLDP. Correcting for both of these spin-down effects we here simply assume  $P = \sqrt{2} P_{\text{eq}}$ . The resulting median values of  $P_{\text{eq}}$  are thus found to be 2.8 ms and 11 ms, respectively. For a  $1.4 M_{\odot}$  neutron star these median equilibrium spin periods correspond to  $\Delta M_{\text{eq}} = 0.06 M_{\odot}$  and  $\Delta M_{\text{eq}} = 0.01 M_{\odot}$  for pulsars with a He WD or a CO WD companion, respectively. In other words, to explain the observed period distribution of these two classes of recycled pulsars we conclude that those pulsars with CO WD companions typically have accreted less mass by a factor of 6, compared to the pulsars with He WD companions. This conclusion remains valid for other scalings between the present spin period,  $P$  and the initial spin period,  $P_{\text{eq}}$  – even for

assuming  $P = P_{\text{eq}}$ . We conclude from Fig. 9 that BMSPs with CO WDs usually have evolved via early Case B or Case C RLO (the latter leading to CE evolution). The reason is that these two paths involve mass transfer on a much shorter timescale, and hence lead to smaller amounts of transferred mass, leading to less effective recycling and thereby longer spin periods, as seen among the observed pulsars in Fig. 9 (see also Section 7). Furthermore, the BMSPs with CO WDs also have relatively large values of  $\dot{P}$ . This reflects larger values of  $B$ , which is expected since less mass was accreted in these systems, cf. Section 4.4.1. The only exception known from the description outlined above is PSR J1614–2230 which is discussed in Section 9.

For BMSPs with He WD companions, we notice from the orbital period distribution in Fig. 3 (central panel) that the majority of these systems seem to have evolved through Case B RLO with an initial LMXB orbital period of  $P_{\text{orb}} > 1$  day (Tauris & Savonije 1999; Podsiadlowski et al. 2002; Tauris 2011, and references therein).

### 6.2 Double neutron star systems

In Fig. 9 we have also plotted the spin distribution of recycled pulsars with neutron star companions and  $P < 100$  ms. These systems originate from high-mass X-ray binaries (HMXBs), e.g. Tauris & van den Heuvel (2006). Their spin distribution is skewed to larger periods compared to the recycled pulsars with CO WD companions. This is expected since their massive stellar progenitors evolved even more rapidly than the donor stars of the IMXBs. It is generally believed that double neutron star systems evolved via a CE and spiral-in phase since the mass transfer in HMXBs is always dynamically unstable – see however Brown (1995); Dewi et al. (2006) for an alternative formation mechanism via a double-core scenario.

### 6.3 Formation of recycled pulsars with $P_{\text{orb}} > 200$ days

As mentioned earlier (see also Fig. 3), pulsars with  $P_{\text{orb}} > 200$  days all have slow rotational spins. This fact could be explained if they had accreted little mass. If their progenitors were wide-orbit LMXBs they had experienced continuous super-Eddington mass transfer on a short timescale of the order 10 Myr (Tauris & Savonije 1999). However, even if their accretion rates had been restricted to the Eddington limit these accreting pulsars could still have received up to  $0.3 M_{\odot}$ . This amount is 10 times larger than needed to spin up a pulsar to 5 ms according to equation (14). Therefore, to explain the slow spin periods of these wide-orbit recycled pulsars one may speculate that the accretion process was highly inefficient due to, for example, enhanced accretion disk instabilities (van Paradijs 1996; Dubus et al. 1999). This could be related to the advanced evolutionary stage of their donor stars on the red giant branch (RGB). These stars had deep convective envelopes which may lead to enhanced clump formation in the transferred material.

Alternatively, one may ask if these systems descended from wide-orbit IMXBs which underwent a CE and a mild spiral-in. In this case their companion stars should be fairly massive CO WDs ( $\geq 0.5 M_{\odot}$ , see fig. 1 in Paper I). However,

quite a few of these wide-orbit recycled pulsars seem to have relatively low-mass He WDs according to their mass functions. In fact it was pointed out by Tauris (1996); Tauris & Savonije (1999); Stairs et al. (2005) that some of those WD masses may even be significantly less massive than expected from the  $(M_{\text{WD}}, P_{\text{orb}})$ -relation which applies to He WDs descending from LMXBs, although this analysis still has its basis in small numbers. It is therefore important to observationally determine the masses of the WDs in these wide-orbit pulsars systems and settle this evolutionary question.

## 7 SPINNING UP POST COMMON ENVELOPE PULSARS

An interesting question is if our derived relation between pulsar spin and accreted mass (equation 14) can also explain the observed spin periods of the BMSPs with *massive* WD companions and short orbital periods, i.e. systems we expect to have evolved through a CE evolution. Let us consider the important system PSR J1802-2124 recently observed by Ferdman et al. (2010). The nature of its  $0.78 \pm 0.04 M_{\odot}$  CO WD companion, combined with an orbital period of 16.8 hr and a post-accretion pulsar mass of only  $1.24 \pm 0.11 M_{\odot}$  makes this one of our best cases for a system which evolved via a CE and spiral-in phase. The present spin period of the pulsar is 12.6 ms. Assuming an initial equilibrium spin period of 10 ms we find from equation (14) that  $\Delta M_{\text{eq}} \simeq 0.01 M_{\odot}$  which is a much more acceptable value for a system undergoing CE-evolution (compared to the  $0.10 M_{\odot}$  needed for spinning up a BMSP with a He WD companion to a spin period of a few ms). However, one still has to account for the  $0.01 M_{\odot}$  accreted. It is quite likely that this accretion occurred *after* the CE-phase and we now consider this possibility.

### 7.1 Case BB RLO in post common envelope binaries

The total duration of the CE-phase itself is probably so short ( $< 10^3$  yr, e.g. Podsiadlowski 2001; Passy et al. 2012; Ivanova et al. 2012) that no substantial accretion onto the neutron star is possible with respect to changing its rotational dynamics – even if the envelope of the donor star is not ejected from the system until long after the in-spiral of the secondary star which occurs on a dynamical timescale of a few  $P_{\text{orb}}$ . Thus we are left with two possibilities: 1) the recycling of the pulsar occurs during the subsequent stable RLO of a naked helium star following the CE (Case BB RLO), or 2) the recycling occurs due to wind accretion from the naked helium or carbon-oxygen core left behind by the donor star after it loses its envelope in the CE-phase.

In Fig. 10 we show one of our model calculations of Case BB RLO. In our example we assumed a  $1.40 M_{\odot}$  helium star ( $Y = 0.98$ ) as the donor and a  $1.35 M_{\odot}$  neutron star as the accretor. The giant phase of a helium star is short lived and in this case the mass transfer lasts for about 170,000 yr. (This time interval, however, is much longer than the CE-event.) Assuming the accretion onto the neutron star to be Eddington limited will therefore lead to an accretion of only about  $7 \times 10^{-3} M_{\odot}$ . Although this is a small amount, it is still

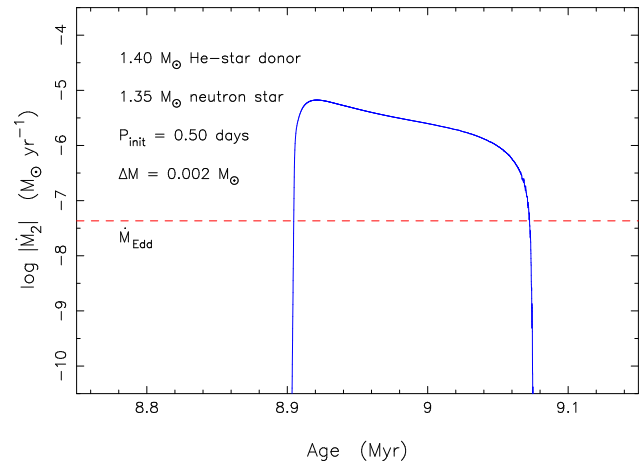


**Figure 10.** A model calculation of Case BB RLO. The plot shows mass-transfer rate as a function of age for a  $1.4 M_{\odot}$  helium star donor. The initial orbital period is 0.50 days and the neutron star mass is  $1.35 M_{\odot}$ . After the RLO the donor star settles as a  $0.89 M_{\odot}$  CO WD orbiting the recycled pulsar with an orbital period of 0.95 days. The mass-transfer phase only lasts for about 170,000 yr. Even if the neutron star only accretes  $\sim 0.002 M_{\odot}$  (assuming an accretion efficiency of just 30%) it is still able to spin up the pulsar to a spin period of 36 ms. If the neutron star accretes all matter at the Eddington limit it can be spun up to 14 ms. A comparison can be made with the observed spin periods of BMSPs with CO WD companions in the bottom panel of Fig. 3.

sufficient to spin up the recycled pulsar to a period of 14 ms, which is even faster than the observed median spin period of BMSPs with CO WD companions (see Fig. 9). Assuming the accretion efficiency to be only 30 per cent of  $\dot{M}_{\text{Edd}}$  would still spin up the pulsar to 36 ms. A helium donor star with a lower mass can even spin up the pulsar below 14 ms. We found that for a  $1.10 M_{\odot}$  helium star donor the neutron star can accrete 50 per cent more (resulting in  $P_{\text{eq}} = 11$  ms) due to the increased nuclear timescale of the shell burning of a lower mass helium star. Hence, based on rotational dynamics we conclude that Case BB RLO is a viable formation channel to explain most of the observed BMSPs with CO WD companions. A more systematic study of Case BB RLO for various system configurations is needed in order to find the minimum possible spin period of BMSPs with CO WD companions formed via this formation channel.

It should be noted that a pulsar may also be recycled via Case BA RLO, i.e. from RLO which is initiated while the companion star is still on the helium main sequence (see Dewi et al. 2002, for detailed calculations). In this case the mass-transfer phase will last up to ten times longer, compared to Case BB RLO, providing more than sufficient material to recycle the pulsar effectively. However, in order to initiate RLO while the helium star donor is still burning core helium on its main sequence requires a tight, fine-tuned interval of orbital separation following the common envelope. Typical orbital periods needed are 1-2 hours. Since Case BB RLO is initiated for a much wider interval of larger orbital periods (up to several tens of days) we expect many more systems to evolve via Case BB RLO compared to Case BA RLO.

### 7.2 Wind accretion prior to Case BB RLO

Finally, we tested if the neutron star could acquire any significant spin up from wind accretion in the epoch between post-CE evolution and Case BB RLO. To produce CO or ONeMg WD remnants via Case BB RLO one would expect a typical helium star mass of  $1.1 - 2.2 M_{\odot}$  prior to the mass transfer. These stars have luminosities of  $\log(L/L_{\odot}) = 2.5 - 3.3$  (Langer 1989) and typically spend less than 10 Myr on the He-ZAMS before they expand and initiate Case BB RLO. Their mass-loss rates are of the order  $\dot{M}_{\text{wind}} \simeq 10^{-10 \pm 0.6} M_{\odot} \text{ yr}^{-1}$  (Jeffery & Hamann 2010). Therefore, even if as much as 10 per cent of this ejected wind mass was accreted onto the neutron star it would accrete a total of at most  $\sim 10^{-4} M_{\odot}$  prior to the RLO. We therefore conclude that wind accretion prior to Case BB RLO is negligible for the recycling process of BMSPs with CO WD companions.

### 7.3 Will the progenitor binaries make it to Case BB RLO?

Before drawing conclusions about the Case BB RLO we should verify that the progenitor binary survives to follow this path. In Paper I we argued Case BB RLO does not work for PSR J1614–2230 because the envelope of the CO WD progenitor star is too tightly bound to be ejected during the spiral-in phase<sup>3</sup>. Is that the case for all BMSPs? The answer is no. We find that if the post-CE orbital period (i.e. the observed  $P_{\text{orb}}$  of a BMSP) is about 0.5 days or less then sufficient orbital energy will be released during spiral in to energetically allow for a successful ejection of the envelope of the original  $5 - 7 M_{\odot}$  red giant donor star. The total (absolute) binding energy of the envelope of such a star is  $1.3 - 2.2 \times 10^{48}$  ergs which is equivalent to an orbital energy corresponding roughly to  $P_{\text{orb}} \leq 0.5$  days. Since we must require  $\Delta E_{\text{orb}} > E_{\text{env}}$  to avoid a merger we therefore conclude that Case BB RLO is in principle a viable formation channel for BMSPs with CO WD companions if these systems have short orbital periods. As argued earlier we consider PSR J1802–2124 (which has  $P_{\text{orb}} = 16.8$  hours) as a strong case for a BMSP which evolved through a common envelope. Whether or not one can finetune the Case BB RLO evolution to account for the recycling of this pulsar, or if the recycling was due to wind accretion from the exposed post-CE CO core of an AGB star or, thirdly, if accretion-induced collapse of an ONeMg WD was at work, is an interesting question to address.

## 8 TRUE AGES OF MILLISECOND PULSARS

Knowledge of the true ages of recycled radio pulsars is important for comparing the observed population with the properties expected from the spin-up theory outlined in Section 4. All radio pulsars lose rotational energy with age and the braking index,  $n$  is given by (Manchester & Taylor 1977):

<sup>3</sup> We even considered a conservative Case BB RLO evolution which is far from valid given that the mass-transfer rate is highly super-Eddington, see Fig. 10 above.

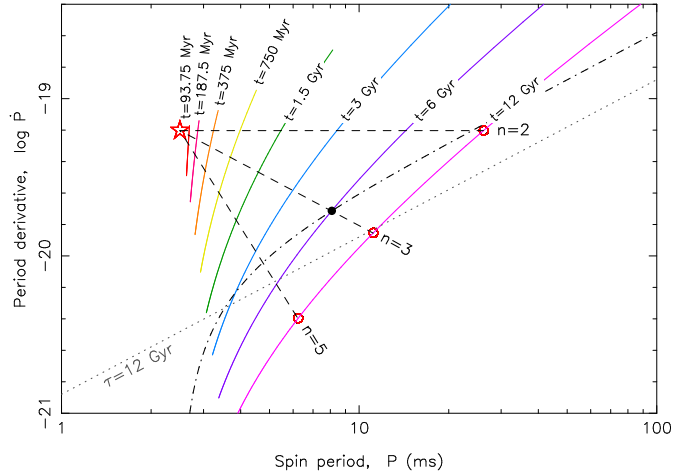


**Figure 11.** Isochrones of pulsar evolution for a pulsar with known initial  $(P_0, \dot{P}_0)$  for different values of a constant braking index,  $n$ . Along any given isochrone  $n$  increases continuously from  $n = 1$  (top) to  $n = 15$  (bottom). The initial position of the recycled test pulsar is shown by a red star and the dashed lines show evolutionary tracks for  $n = 2, 3$  or  $5$ , respectively. The dotted line yields a characteristic age,  $\tau \equiv P/(2\dot{P})$  of 12 Gyr. This line would intersect with the 12 Gyr isochrone exactly at  $n = 3$  if  $P_0 \ll P$ , which is not completely fulfilled. The dot-dashed isochrone line is a general solution to equation (23) for  $n = 3$ ,  $t = 6$  Gyr and  $P_0 = 2.5$  ms, but unknown  $\dot{P}_0$ .

$$\dot{\Omega} \propto -\Omega^n \quad (21)$$

which yields (for  $n$  constant):  $n \equiv \Omega \dot{\Omega} / \dot{\Omega}^2$ . This deceleration law can also be expressed as:  $\dot{P} \propto P^{2-n}$  and hence the slope of a pulsar evolutionary track in the  $P\dot{P}$ -diagram is simply given by:  $2 - n$ . Depending on the physical conditions under which the pulsar spins down  $n$  can take different values as mentioned earlier. For example:

gravitational wave radiation	$n = 5$
B-decay or alignment or multipoles	$n > 3$
perfect magnetic dipole	$n = 3$
B-growth/distortion or counter-alignment	$n < 3$

(22)

The combined magnetic dipole and plasma current spin-down torque may also result in  $n \neq 3$  (Contopoulos & Spitkovsky 2006). A simple integration of equation (21) for a *constant* braking index ( $n \neq 1$ ) yields the well-known expression:

$$t = \frac{P}{(n-1)\dot{P}} \left[ 1 - \left( \frac{P_0}{P} \right)^{n-1} \right] \quad (23)$$

where  $t$  is the so-called true age of a pulsar, which had an initial spin period  $P_0$  at time  $t = 0$ .

### 8.1 Isochrones in the $P\dot{P}$ -diagram

Unfortunately, one cannot directly use the equation above to obtain evolutionary tracks in the  $P\dot{P}$ -diagram (even under the assumption of a constant  $n$  and a known initial spin period,  $P_0$ ). For chosen values of  $t$ ,  $n$  and  $P_0$  one can find a whole family of solutions  $(P, \dot{P})$  to be plotted as an isochrone, see the dot-dashed line in Fig. 11 (and see also

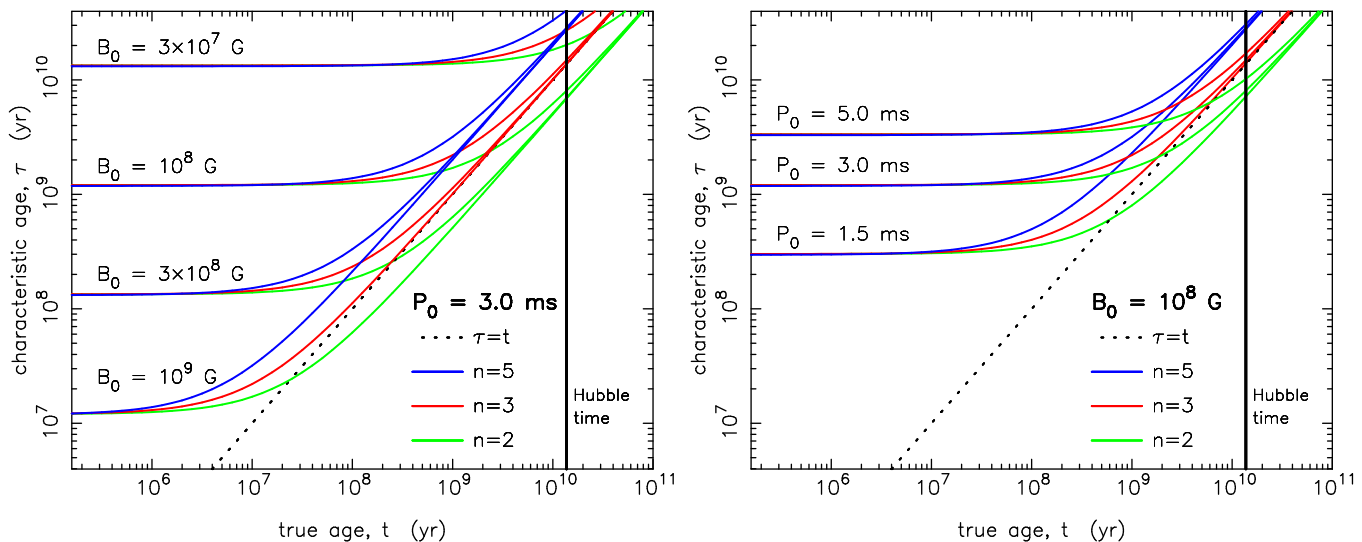


**Figure 12.** Evolutionary tracks of characteristic ages,  $\tau$  calculated as a function of true ages,  $t$  for recycled pulsars with a constant braking index of  $n = 2$ ,  $n = 3$ , and  $n = 5$ . In all cases for  $n$  we assumed a constant  $M = 1.4 M_{\odot}$ ,  $\sin \alpha = 1$ , a constant moment of inertia,  $I$  and for  $n = 5$  we also assumed a constant ellipticity,  $\varepsilon \neq 0$ . In the left panel we assumed in all cases an initial spin period of  $P_0 = 3.0$  ms and varied the value of the initial surface magnetic flux density,  $B_0$ . In the right panel we assumed in all cases  $B_0 = 10^8$  G and varied  $P_0$ . The dotted line shows a graph for  $\tau = t$  and thus only pulsars located on (near) this line have characteristic ages as reliable age indicators. We notice that recycled pulsars with small values of  $P_0$ , resulting from either small values of  $B_0$  (left panel) and/or large values of  $P_0$  (right panel), tend to have  $\tau \gg t$ , even at times exceeding the age of the Universe. In all degeneracy splittings of the curves the upper curve (blue) corresponds to  $n = 5$ , the central curve (red) corresponds to  $n = 3$  and the lower curve (green) corresponds to  $n = 2$ . The asymptotic behavior of the curves can easily be understood from equation (25) – see text for explanations.

Kiziltan & Thorsett 2010). However, there is only one point which is a valid solution for a given pulsar and the above equation does reveal which point is correct. The problem is that the variables in equation (23) are not independent and we do not know a priori the initial spin period derivative,  $\dot{P}_0$ . The evolution of the spin period is a function of both  $t$ ,  $n$ , the initial period and its time derivative, i.e.  $P(t, n, P_0, \dot{P}_0)$ . Here, for simplicity, we assume  $n$  to be constant. To determine  $\dot{P}_0$  one must make assumptions about the initial surface magnetic flux density,  $B_0$ , the initial magnetic inclination angle,  $\alpha_0$  and the initial ellipticity,  $\varepsilon_0$  (the geometric distortion which is relevant for rotational deceleration due to gravitational wave radiation). Once  $\dot{P}_0$  is known, one can combine equation (23) with the deceleration law, e.g.  $\dot{P}P^{n-2} = \text{const.}$  (equation 21), and solve by integration for the evolution of a given pulsar. This way one can produce isochrones, for example as a function of the braking index for pulsars with the same given value of  $\dot{P}_0$ .

In Fig. 11 we have plotted pulsar isochrones for a pulsar with  $P_0 = 2.5$  ms and  $\dot{P}_0 = 6.26 \times 10^{-20}$  (e.g., corresponding to  $B_0 = 1.15 \times 10^8$  G for  $M = 1.4 M_{\odot}$ ,  $\sin \alpha_0 = 1$  and  $\varepsilon_0 = 0$ ) by varying the value of the braking index such that  $1 \leq n \leq 15$ . Our numerical calculations were confirmed by analytic calculations for the special cases where  $n = 2, 3$  or  $5$  (see small circles at the  $t = 12$  Gyr isochrone). The black dot indicates where the two 6 Gyr isochrones, calculated for  $n = 3$  or  $\dot{P}_0 = 6.26 \times 10^{-20}$ , respectively, cross each other for a common solution and also in conjunction with the intersection of the evolutionary track calculated for the same values of  $n$  and  $\dot{P}_0$ .

## 8.2 Characteristic versus true ages of MSPs

Introducing the characteristic age of a pulsar,  $\tau \equiv P/(2\dot{P})$  one finds the relation between  $\tau$  (the observable) and  $t$ :

$$\log \tau = \log t + \log \left( \frac{n-1}{2} \right) - \log \left( 1 - \left( \frac{P_0}{P} \right)^{n-1} \right) \quad (24)$$

for evolution with a constant braking index,  $n$ . The asymptotic version of this relation (as  $t \rightarrow \infty$  and  $P \gg P_0$ ) is given by:

$$\log \tau = \begin{cases} \log t + \log 2 & \text{for } n = 5 \\ \log t & \text{for } n = 3 \\ \log t - \log 2 & \text{for } n = 2 \end{cases} \quad (25)$$

In Fig. 12 we have plotted  $\tau$  as a function of  $t$  on log-scales for braking indices of  $n = 2, 3$  and  $5$ , respectively. Initially, when  $t$  is small and  $P \simeq P_0$ ,  $\tau$  is always greater than  $t$ . After a certain timescale  $\tau$  can either remain larger or become smaller than  $t$ , depending on  $n$ . For  $n = 5$  ( $n > 3$ ) we always have  $\tau > t$ , for  $n = 3$  we have  $\tau \geq t$  and only for  $n = 2$  ( $n < 3$ ) we have the possibility that  $\tau$  can be either greater or smaller than  $t$ . Having  $n = 2$  corresponds to  $\dot{P}$  being a constant, and solving for  $\tau = t$  yields  $P = 2P_0$  and  $t = P_0/\dot{P}$ . We notice that for a reasonable interval of braking index values  $2 \leq n \leq 5$  the observed characteristic age will never deviate from the true age by more than a factor of two when  $P \gg P_0$ . However, to reach  $P \gg P_0$  may take several Hubble timescales if  $B_0$  is low.

The characteristic age at birth (after recycling) is given by:  $\tau_0 = P_0/(2\dot{P}_0)$  and combining with equation (5) we get:

$$\tau_0 = \frac{P_0^2 k^2}{2B_0^2} \quad (26)$$

where the constant  $k = 9.2 \times 10^{18} \text{ G s}^{-1/2}$  for  $\sin \alpha_0 = 1$  and  $M = 1.4 M_\odot$ . This expression verifies the well-known result that MSPs that are born relatively slowly spinning (large  $P_0$  value) and/or have a relatively weak initial  $B$ -field (small  $B_0$  value) are also those MSPs which are born with characteristic ages which differ the most from their true ages as shown in Fig. 12 (see also Kiziltan & Thorsett 2010). In other words, those pulsars with smallest values of  $\dot{P}_0$  for a given  $B_0$  or  $P_0$  are those with  $\tau_0 \gg t$  (which is hardly a surprise given that  $\tau \equiv P/(2\dot{P})$ ). The extent to which they continue evolving with  $\tau \gg t$  depends on their initial conditions ( $P_0, B_0$ ) and well as  $n$ . Notice, for recycled pulsars  $n$  is not measurable and for this reason its value remains unknown.

### 8.3 Comparison with observations

#### 8.3.1 Kinematic corrections to $\dot{P}$

In a discussion of the ages and the evolution of millisecond pulsars in the  $P\dot{P}$ -diagram kinematic corrections must be included when considering the observed values of  $\dot{P}$  ( $\dot{P}_{\text{obs}}$ ). The kinematic corrections to the intrinsic  $\dot{P}$  ( $\dot{P}_{\text{int}}$ ) are caused by acceleration due to proper motion of nearby pulsars (Shklovskii 1970) and to vertical ( $a_Z$ ) and differential rotational acceleration in our Galaxy ( $a_{\text{GDR}}$ ). The total corrections are given by:

$$\left(\frac{\dot{P}_{\text{obs}}}{P}\right) = \left(\frac{\dot{P}_{\text{int}}}{P}\right) + \left(\frac{\dot{P}_{\text{shk}}}{P}\right) + \frac{a_Z}{c} + \frac{a_{\text{GDR}}}{c} \quad (27)$$

and following Damour & Taylor (1991) and Wolszczan et al. (2000) we can express these corrections as:

$$\begin{aligned} \left(\frac{\dot{P}_{\text{obs}}}{P}\right) &= \left(\frac{\dot{P}_{\text{int}}}{P}\right) + \frac{\mu^2 d}{c} - \frac{a_Z \sin b}{c} \\ &- \frac{v_0^2}{cR_0} \left[ \cos l + \frac{(d/R_0) - \cos l}{1 + (d/R_0)^2 - 2(d/R_0) \cos l} \right] \end{aligned} \quad (28)$$

where  $d$  is the distance to the pulsar,  $\mu$  is the proper motion (related to the transverse velocity,  $v_\perp = \mu d$ ),  $a_Z$  is the vertical component of Galactic acceleration (e.g., from the Galactic potential model of Kuijken & Gilmore (1989)),  $l$  and  $b$  are the Galactic coordinates of the pulsar,  $R_0 = 8.0 \text{ kpc}$  and  $v_0 = 220 \text{ km s}^{-1}$  represent the distance to the Galactic centre and the orbital velocity of the Sun, and  $c$  is the speed of light in vacuum. The corrections to  $\dot{P}$  due to Galactic vertical and differential rotational accelerations are typically quite small (a few  $10^{-22} \ll \dot{P}_{\text{int}}$ ) and can be ignored, except in a few cases (see below).

#### 8.3.2 Evolutionary tracks and true age isochrones

In order to investigate if we can understand the distribution of MSPs in the  $P\dot{P}$ -diagram we have traced the evolution of eight hypothetical, recycled MSPs with different birth locations. In each case we traced the evolution for  $2 \leq n \leq 5$  and plotted isochrones similar to those introduced in Fig. 11. The results are shown in Fig. 13 together with observed data. All the measured  $\dot{P}$  values have been corrected for kinematic effects, as described above. If the transverse velocity of a given pulsar is unknown we used a value of  $67 \text{ km s}^{-1}$  which we found to be the median

value of the 49 measured velocities of binary pulsars<sup>4</sup>. In five cases (PSRs: J1231–1411, J1614–2230, J2229+2643, J1024–0719, J1801–1417, marked in squares in Fig. 13) we obtain  $\dot{P}_{\text{int}} < 0$  which is not physically possible. The reason is probably an overestimate of the pulsar distance. In those cases we have recalculated  $\dot{P}_{\text{int}}$  assuming only half the distance and included the corrections due to Galactic vertical and differential rotational acceleration.

Three main conclusions can be drawn from this diagram:

1) The overall distribution of observed pulsars follows nicely the banana-like shape of an isochrone with multiple choices for  $\dot{P}_0$  (or  $B_0$ ), see fat purple line. The chosen values of  $P_0 = 3.0 \text{ ms}$ ,  $n = 3$  and  $t = 6 \text{ Gyr}$  are just for illustrative purposes only and not an attempt for a best fit to the observations. Fitting to one curve would not be a good idea given that MSPs are born with different initial spin periods, which depend on their accretion history, and given that the pulsars have different ages. The spread in the observed population is hinting that recycled pulsars are born at many different locations in the  $P\dot{P}$ -diagram.

2) The far majority of the recycled pulsars seem to have true ages between 3 and 12 Gyr, as expected since the population accumulates and the pulsars keep emitting radio waves for a Hubble time.

3) Pulsars with small values of the period derivative  $\dot{P} \simeq 10^{-21}$  hardly evolve at all in the diagram over a Hubble time. This is a trivial fact, but nevertheless important since it tells us that these pulsars were basically born with their currently observed values of  $P$  and  $\dot{P}$  (first pointed out by Camilo et al. 1994). In this respect, it is interesting to notice PSR J1801–3210 (recently discovered by Bates et al. 2011) which must have been recycled with a relatively slow birth period,  $P_0 \sim 7 \text{ ms}$  despite its low  $B$ -field  $< 10^8 \text{ G}$  – see Fig. 5 for its location in the  $P\dot{P}$ -diagram.

One implication of the third conclusion listed above is that some radio MSPs must have been born with very small values of  $B_0 \simeq 1 \times 10^7 \text{ G}$ , if the inferred  $B$ -fields using equation (5) are correct. Given their weak  $B$ -fields such sources would most likely not be able to channel the accreted matter sufficiently to become observable as AXMSPs (Wijnands & van der Klis 1998). One case is the 1.88 ms radio pulsar J0034–0534 (Bailes et al. 1994) which has an observed  $\dot{P} = 4.97 \times 10^{-21}$ . However, this pulsar has a transverse velocity of  $146 \text{ km s}^{-1}$  and correcting for the Shklovskii effect yields an intrinsic period derivative of only  $\dot{P}_{\text{int}} = 5.36 \times 10^{-22}$ . These values result in  $B = 9 \times 10^6 \text{ G}$  (for  $M = 1.4 M_\odot$  and  $\alpha = 90^\circ$ ) and a characteristic age,  $\tau = 55 \text{ Gyr}$ . Once again we see that  $\tau$  is not a good measure of the true age of a pulsar. If this pulsar has any gravitational wave emission ( $\varepsilon \neq 0$ ) its derived surface  $B$ -field would be even smaller. We also notice a few pulsars which seem to have been recycled with  $\dot{M} < 10^{-3} \dot{M}_{\text{Edd}}$  (approaching  $10^{-4} \dot{M}_{\text{Edd}}$ ). Their progenitors could be the so-called weak LMXBs which are low-luminosity LMXBs (van der Klis 2006). It is also quite possible that their po-

<sup>4</sup> If we add to this sample the measured velocities of 13 isolated pulsars which show strong signatures of being recycled ( $P < 100 \text{ ms}$  and  $\dot{P} < 10^{-16}$ ) the median velocity becomes  $69 \text{ km s}^{-1}$ , which would make the Shklovskii corrections slightly larger and thus  $\dot{P}_{\text{int}}$  somewhat smaller.

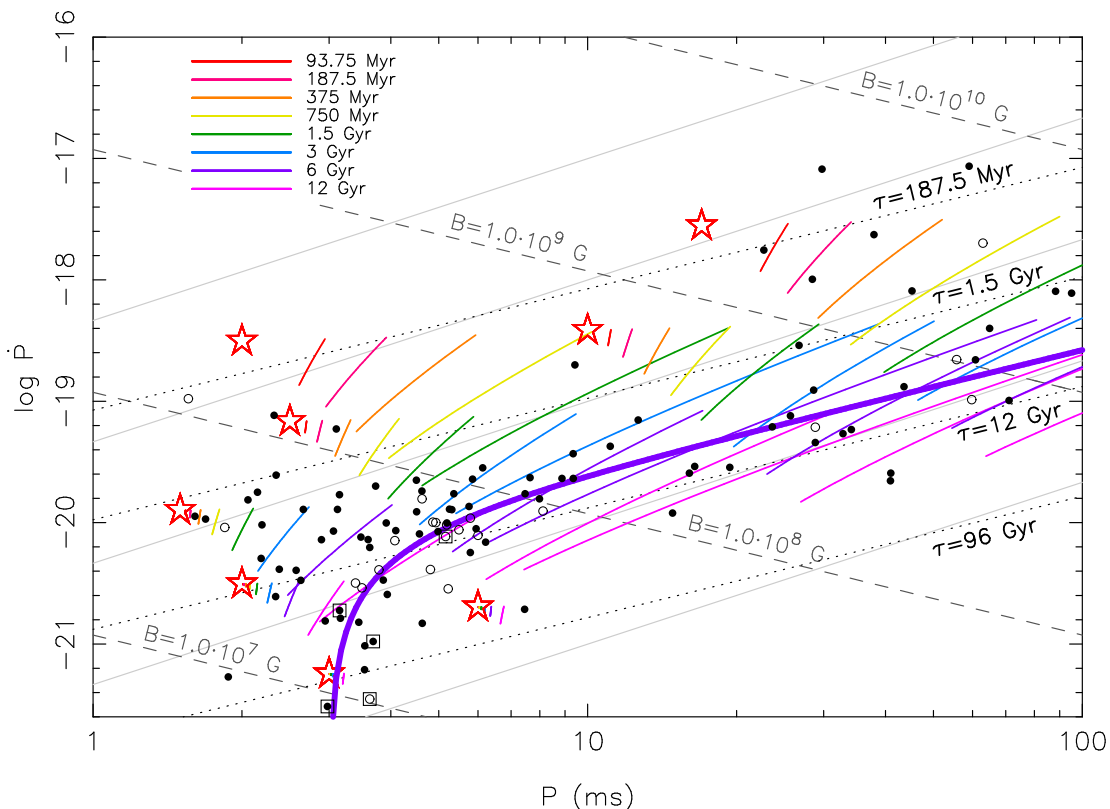


**Figure 13.** Isochrones of eight hypothetical recycled pulsars born at the locations of the red stars. The isochrones were calculated for different values of the braking index,  $2 \leq n \leq 5$  (see Fig. 11 for details). Also plotted are inferred  $B$ -field values (dashed lines) and characteristic ages,  $\tau$  (dotted lines). The thin grey lines are spin-up lines with  $\dot{M}/\dot{M}_{\text{Edd}} = 1, 10^{-1}, 10^{-2}, 10^{-3}$  and  $10^{-4}$  (top to bottom, and assuming  $\sin \alpha = \phi = \omega_c = 1$ ). In all calculations we assumed a pulsar mass of  $1.4 M_{\odot}$ . It is noted that the majority of the observed population is found near the isochrones for  $t = 3 - 12$  Gyr, as expected. The fat, solid purple line indicates an example of a  $t = 6$  Gyr isochrone for pulsars with any value of  $P_0$ , but assuming  $P_0 = 3.0$  ms and  $n = 3$ . It is seen how the banana shape of such a type of an isochrone fits very well with the overall distribution of observed pulsars in the Galactic disk. Binary pulsars are marked with solid circles and isolated pulsars are marked with open circles. All values of  $\dot{P}$  have been corrected for the Shklovskii effect using data from the *ATNF Pulsar Catalogue*. Pulsars in squares have been corrected for both a reduced distance and acceleration effects in the Galaxy. Pulsars with very small values of  $\dot{P}$  are basically born on location in this diagram since their evolutionary timescale exceeds the Hubble time. Pulsars with relative small values of  $P$  and large values of  $\dot{P}$  have the potential to constrain white dwarf cooling models – see text for discussion.

sition in the  $P\dot{P}$ -diagram was strongly shifted during the RLDP (see fig. 2 in Tauris 2012) so that their average mass-accretion rate could have been larger prior to the RLDP. Alternatively, these MSPs demonstrate that  $\phi > 1$  and  $\omega_c < 1$  which could move the spin-up line substantially downwards, as demonstrated in Fig. 5.

It is obvious that a different sample of recycled pulsar birth locations in Fig. 13 would lead to somewhat different isochrones. However, we believe the qualitative interpretation is trustworthy and encourage further detailed statistical population analysis to be carried out (see Kiziltan & Thorsett 2010).

It is worth pointing out the difference in evolutionary timescales for the progenitor systems of BMSPs with He WDs or CO WDs, respectively. The IMXBs, leading mainly to BMSPs with CO WD companions, evolve on nuclear timescales of typically 100–300 Myr. Hence, BMSPs with CO WDs could have true ages from zero to up to about 12 Gyr (assuming the first progenitor stars in our Galaxy formed  $\sim 1$  Gyr after Big Bang). The LMXBs, on the other hand, could easily have ages of 10 Gyr *before* they form,

which is the typical timescale for a  $1 M_{\odot}$  star to evolve into a sub-giant which fills its Roche-lobe in an orbit with  $P_{\text{orb}}$  larger than a few days. One may then think that BMSPs with He WD companions must be much younger than BMSPs with CO WD companions (the BMSP age being calculated from after the RLDP). However, some LMXBs may have donor stars up to  $2 M_{\odot}$  and these stars evolve on a timescale of only  $\sim 1.5$  Gyr. Hence, BMSPs with He WD companions can have almost similar true (post recycling) ages as BMSPs with CO WD companions.

### 8.3.3 PSR B1937+21 and PSR J0218+4232: two recently fully recycled pulsars?

Although recycled pulsars with high values of  $\dot{P}$  evolve fast across the  $P\dot{P}$ -diagram, we should expect to observe a few fully recycled pulsars with  $\dot{P} \simeq 10^{-19}$ . The only two cases in the Galactic disk known so far are PSR B1937+21 (Backer et al. 1982) and PSR 0218+4232 (Navarro et al. 1995), see Fig. 5. The latter is a 2.32 ms pulsar ( $\dot{P}_{\text{int}} = 7.66 \times 10^{-20}$ ) which not only has a small

characteristic age ( $\tau = 480$  Myr) but also must have a fairly young *true* age. Even if we assume it evolved with a constant value of  $\dot{P}$  (and disregard the possibility of  $n > 2$  which would have resulted in a larger initial value of  $\dot{P}_0$  and hence a younger age) we find  $t = 132 - 546$  Myr when assuming  $P_0$  is in the interval 1–2 ms. As expected, this system hosts a white dwarf companion star which is still hot enough to be detected. Interestingly enough, all the cooling models applied by Bassa et al. (2003) to this white dwarf seem to indicate a somewhat larger age (see their fig. 4). This discrepancy has the intriguing consequence that either their applied cooling models are overestimating the age of the white dwarf, or this pulsar evolved with  $n < 2$  and evolved *upward* in the  $P\dot{P}$ -diagram.

PSR B1937+21 is the first MSP discovered and is not only young, like PSR J0218+4232, but also isolated. This fast spinning pulsar (1.56 ms) has  $\dot{P}_{\text{int}} = 1.05 \times 10^{-19}$  which yields a characteristic age of  $\tau = 235$  Myr. We find upper limits ( $n = 2$ ) for the true age to be in the interval  $t = 78 - 229$  Myr when assuming  $P_0$  is in the interval 0.8–1.3 ms. MSPs (or any pulsar with a low  $\dot{P}$ ) are not believed to be formed directly from supernova explosions. They must interact with a companion star to spin up and decrease their B-field by a large amount. Thus it is interesting that this pulsar was able to evaporate its companion star within a timescale of (a few)  $10^8$  yr – unless it evolved from an ultra-compact X-ray binary possibly initially leaving a planet around it (van Haaften et al. 2012).

### 8.3.4 PSR J1841+0130: a young mildly recycled pulsar

PSR J1841+0130 is the 29 ms binary pulsar discussed earlier in Section 3.2.1. It has an unusually high value of  $\dot{P}$ , close to  $10^{-17}$ , which reveals that it is young and places it close to the spin-up line for  $\dot{M} = \dot{M}_{\text{Edd}}$  (assuming  $\sin \alpha = \phi = \omega_c = 1$ ), see Fig. 5. The characteristic age of PSR J1841+0130 is 58 Myr. An upper limit to its true age is 77 Myr, which is found by assuming  $n = 2$  and  $P_0 = 10$  ms ( $P_0$  cannot have been much smaller than 10 ms under the above mentioned assumptions regarding the spin-up line). If we assume  $n = 3$ , the upper limit for the true age is 51 Myr. The WD companion is therefore hot enough to yield spectroscopic information that will reveal its true nature – i.e. whether this is a CO WD or a He WD, as discussed in Section 3.2.1. According to the dispersion measure,  $DM = 125 \text{ cm}^{-3} \text{ pc}$ , of this pulsar its distance is about 3 kpc which might make such observations difficult.

## 9 SPINNING UP PSR J1614–2230

Recent Shapiro delay measurements of the radio millisecond pulsar J1614–2230 (Demorest et al. 2010) allowed a precise mass determination of this record high-mass neutron star and its white dwarf companion. A few key characteristic parameters of the system are shown in Table 3. In Paper I we discussed the binary evolution which led to the formation of this system (see also Lin et al. 2011). For estimating the amount of necessary mass accreted in order to recycle PSR J1614–2230 we can apply equation (14) and assuming, for example, an initial spin period of 2.0 ms following the

**Table 3.** Selected physical parameters of the binary millisecond pulsar J1614–2230 (data taken from Demorest et al. 2010).

Parameter	value
Pulsar mass	$1.97 \pm 0.04 M_{\odot}$
White dwarf mass	$0.500 \pm 0.006 M_{\odot}$
Orbital period	8.6866194196(2) days
Orbital eccentricity	$1.30 \pm 0.04 \times 10^{-6}$
Pulsar spin period	3.1508076534271 ms
Period derivative	$9.6216 \times 10^{-21}$

RLO. We find that  $\Delta M_{\text{eq}} = 0.11 M_{\odot}$ . This result is in fine accordance with our Case A calculation in Paper I where a total of  $0.31 M_{\odot}$  is accreted by the neutron star. (Recall that  $\Delta M_{\text{eq}}$  is a minimum value for ideal, efficient spin up.) For the Case C scenario it is difficult to reconcile the required accretion of  $0.11 M_{\odot}$  with the very small amount which is expected to be accreted by the neutron star evolving through a CE-phase (usually assumed to be  $\ll 10^{-2} M_{\odot}$ ). Furthermore, in Paper I we argued that Case BB RLO (stable RLO from a naked helium star following a CE) was not an option for this system.

The next check is to see if the spin-relaxation time scale was shorter than the mass-transfer timescale for PSR J1614–2230. In order to estimate  $t_{\text{torque}}$  we must have an idea of the B-field strength during the RLO. Since we have shown in Paper I that the mass-transfer rate in the final phase AB was near (slightly above) the Eddington limit, the value of  $B$  prior to phase AB must have been somewhat larger than its current estimated value of  $\sim 8.4 \times 10^7$  G, according to equation (5). Using  $B = 4 - 10 \times 10^8$  G we find  $t_{\text{torque}} \simeq 2 - 9$  Myr. Since this timescale is shorter than the duration of RLO ( $\sim 10$  Myr for phase AB, see Paper I) we find that indeed it was possible for PSR J1614–2230 to spin up to its equilibrium period.

Based on both binary evolution considerations (Paper I) and the spin dynamics (this paper) we conclude that the Case A scenario is required to explain the existence of PSR J1614–2230. From Fig. 9 we notice that PSR J1614–2230 is an anomaly among the population of BMSPs with CO WD companions – it has an unusual rapid spin. This is explained by its formation via a stable and relatively long lasting IMXB Case A RLO (Paper I) which is, apparently, not a normal formation scenario for these systems.

### 9.1 Evolution of PSR J1614–2230 in the $P\dot{P}$ -diagram

We have demonstrated in Paper I that PSR J1614–2230 mainly accreted its mass during the final phase (AB) of mass transfer. As mentioned above, in this phase the mass-transfer rate was high enough that the accretion onto the neutron star was limited by the Eddington limit, i.e.  $\dot{M} = \dot{M}_{\text{Edd}}$ . A natural question to address (see also Bhalerao & Kulkarni (2011)) is then how PSR J1614–2230 evolved to the present location in the  $P\dot{P}$ -diagram which, at first sight, is even below the spin-up line expected for  $\dot{M} = 10^{-2} \dot{M}_{\text{Edd}}$ . However, one must bear in mind the de-



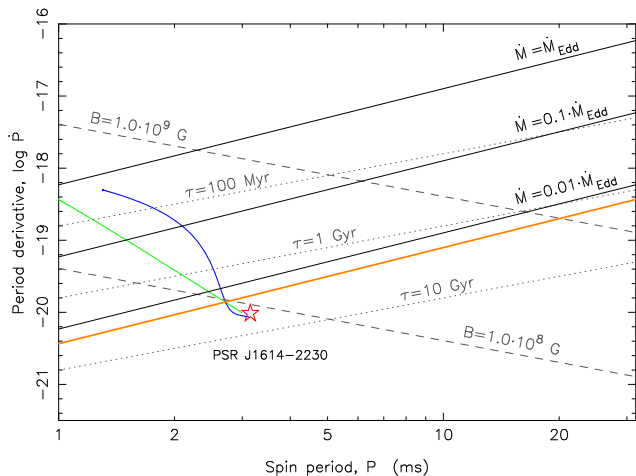


**Figure 14.** Simple models of how PSR J1614–2230 could have evolved from a birth near a spin-up line with  $\dot{M} = \dot{M}_{\text{Edd}}$  to its currently observed location, shown by the red star, within 2 Gyr. The orange line indicates the location of the  $\dot{M} = \dot{M}_{\text{Edd}}$  spin-up line if  $\alpha = 10^\circ$ ,  $\phi = 1.4$  and  $\omega_c = 0.25$ . PSR J1614–2230 is located close to this line which suggests it was born (recycled) close to it. The three black solid lines were calculated by using  $\alpha = 90^\circ$ ,  $\phi = 1$  and  $\omega_c = 1$ . If PSR J1614–2230 was born near such a spin-up line with  $\dot{M} = \dot{M}_{\text{Edd}}$  the need for subsequent spin-down after its birth would be severe and we have evolved a couple of toy models for this alternative: The green model represents gravitational wave radiation and the blue model represents a phase of enhanced torque decay (see text).

pendency of the parameters  $\alpha$ ,  $\phi$  and  $\omega_c$  when discussing the location of the spin-up line (cf. Section 4.3).

If PSR J1614–2230 has a magnetic inclination angle,  $\alpha < 90^\circ$ , and in case  $\phi \approx 1.4$  and  $\omega_c \approx 0.25$ , then the problem is solved since the  $\dot{M} = \dot{M}_{\text{Edd}}$  spin-up line (see orange line in Fig. 14) moves close to the current position of PSR J1614–2230. Therefore we do not see any reason to question the recycling model of BMSPs, based on the observations of the PSR J1614–2230 system, as proposed by Bhalerao & Kulkarni (2011). However, if  $\phi \approx \omega_c \approx 1$  and  $\alpha \approx 90^\circ$  then we have to consider an alternative explanation which we shall now investigate.

It is well-known that the rotational evolution of millisecond pulsars is rather poorly understood since the braking index only has been measured accurately for a few young, non-recycled pulsars. As briefly mentioned in Section 8 there is a variety of mechanisms which can influence the braking index of a pulsar. For example, the geometry of the B-field, the decay of the B-field, a changing magnetic inclination angle (i.e. between the spin axis and the B-field axis of the neutron star), the dynamics of the current flow in the pulsar magnetosphere and gravitational wave emission, e.g. Manchester & Taylor (1977) and Contopoulos & Spitkovsky (2006). We have made a simple toy model for two of these mechanisms to show that PSR J1614–2230 could in principle have accreted with  $\dot{M} = \dot{M}_{\text{Edd}}$  for  $\sin \alpha \approx \phi \approx \omega_c \approx 1$  and subsequently evolve to its presently observed values of  $P$  and  $\dot{P}$  (near the corresponding  $\dot{M} = 10^{-2} \dot{M}_{\text{Edd}}$  spin-up line) after the radio pulsar turned on. In the first model we assumed pulsar spin-down as a result of gravitational wave radiation, which corresponds to  $n = 5$ . The emission of grav-

itational waves is caused by a time-varying quadrupole moment which arises, for example, if the accretion onto the neutron star created non-axisymmetric moments of inertia relative to the spin axis (Shapiro & Teukolsky 1983). In the second model we assumed an enhanced torque decay ( $n > 3$ ) for a limited amount of time following the recycling phase. Such enhanced torque decay could be caused by either alignment between the B-field axis and the spin axis of the pulsar (but not complete alignment, in which case no pulsar would be seen) or further decay of the surface B-field through some unspecified mechanism. In our calculation for the second model we assumed that effectively  $B$  or  $\sin \alpha$  decreased by a factor of about five on a decay timescale of 200 Myr. In Fig. 14 we show that the present position in  $P\dot{P}$ -diagram can be reached from such toy models within 2 Gyr, which is in accordance with the cooling age of the CO WD inferred by Bhalerao & Kulkarni (2011). Notice, if PSR J1614–2230 accreted  $0.31 M_\odot$ , as suggested in Paper I, it would in principle be possible for it to spin up to a period of 0.92 ms (disregarding possible braking torque effects due to gravitational wave radiation, Bildsten (1998)) and thus the initial spin periods in our toy models are justified. However, we emphasize again that it is much less cumbersome to explain the current location of PSR J1614–2230 in the  $P\dot{P}$ -diagram simply by finetuning, in particular,  $\phi$  and  $\omega_c$ . Therefore, future observations of systems like PSR J1614–2230 may help to constrain the disk-magnetosphere interactions.

## 10 NEUTRON STAR BIRTH MASSES

In Paper I, we concluded that the neutron star in PSR J1614–2230 must have been born in a supernova explosion (SN) with a mass of  $1.7 \pm 0.15 M_\odot$  if it subsequently evolved through an X-ray phase with Case A RLO. Based on evolutionary considerations we also found an alternative scenario where the post-SN system could have evolved via Case C RLO leading to a CE. However, we also argued that the CE scenario was less probable given the difficulties in the required evolution from the ZAMS to the X-ray phase. In this paper we rule out the CE scenario completely in view of our analysis of the rotational dynamics. The in-spiral of the neutron star in a CE occurs on such a short timescale that no significant spin up is possible, and wind accretion from the proto WD cannot recycle the pulsar to a spin period of 2–3 ms which requires accretion of  $0.1 M_\odot$ . Recycling via a Case BB RLO, following CE evolution initiated while the progenitor of the donor star was on the RGB, is also not possible for PSR J1614–2230 since its orbital period is so large that its post-CE orbit must have been wide too and thus there could not have been released enough orbital energy during the in-spiral to eject the envelope. Does such a high birth mass of  $1.7 M_\odot$  significantly exceed the neutron star birth masses in previously discovered radio pulsar systems? Below we test if other pulsars may have been born in a SN with a similarly high mass.

The interval of known radio pulsar masses ranges from  $1.17 M_\odot$  in the double neutron star binary PSR J1518+4909 ( $3\sigma$  upper limit, Janssen et al. 2008) to  $1.97 M_\odot$  in PSR J1614–2230, discussed in this paper. Prior to the measurement of PSR J1614–2230 the highest mass inferred for the birth mass of a radio pulsar was only  $1.44 M_\odot$

**Table 4.** Measured masses of neutron stars in NS-WD systems in the Galactic disk, including PSR J1903+0327. The spin periods in the second column are in ms. The third, fourth and fifth column state the measured mass, the minimum accreted mass needed to spin up the pulsar using equation (14) and the derived upper value for its birth mass,  $M_{\text{NS,max}}^{\text{birth}} = M_{\text{NS}} - \Delta M_{\text{eq}}$ , respectively. All masses are in quoted in  $M_{\odot}$ . All error bars are  $1\text{-}\sigma$  values.

Pulsar	$P_{\text{spin}}$	$M_{\text{NS}}$	$\Delta M_{\text{eq}}$	$M_{\text{NS,max}}^{\text{birth}}$
J0437–4715 <sup>1</sup>	5.76	$1.76 \pm 0.20$	0.04	$1.72 \pm 0.20$
J0621+1002 <sup>2</sup>	28.9	$1.70^{+0.10}_{-0.17}$	0.005	$1.70 \pm 0.14$
J0751+1807 <sup>2</sup>	3.48	$1.26 \pm 0.14$	0.07	$1.19 \pm 0.13$
J1012+5307 <sup>3</sup>	5.26	$1.64 \pm 0.22$	0.05	$1.59 \pm 0.21$
J1141–6545 <sup>4</sup>	394	$1.27 \pm 0.01$	—	$1.27 \pm 0.01$
J1614–2230 <sup>5</sup>	3.15	$1.97 \pm 0.04$	0.09	$1.88 \pm 0.04$
J1713+0747 <sup>6</sup>	4.57	$1.53^{+0.08}_{-0.06}$	0.05	$1.48 \pm 0.07$
J1738+0333 <sup>7</sup>	5.85	$1.46^{+0.06}_{-0.05}$	0.04	$1.42 \pm 0.05$
J1802–2124 <sup>8</sup>	12.6	$1.24 \pm 0.11$	0.01	$1.23 \pm 0.11$
B1855+09 <sup>9</sup>	5.36	$1.57^{+0.12}_{-0.11}$	0.04	$1.53 \pm 0.11$
J1903+0327 <sup>10</sup>	2.15	$1.667 \pm 0.021$	0.15	$1.52 \pm 0.02$
J1909–3744 <sup>11</sup>	2.95	$1.44 \pm 0.02$	0.09	$1.35 \pm 0.02$
B2303+46 <sup>12</sup>	1066	$1.38^{+0.06}_{-0.10}$	—	$1.38 \pm 0.08$

References: (1) Verbiest et al. (2008), (2) Nice et al. (2008), (3) Callanan et al. (1998), (4) Bhat et al. (2008), (5) Demorest et al. (2010), (6) Splaver et al. (2005), (7) Antoniadis et al. (2012), (8) Ferdman et al. (2010), (9) Nice et al. (2003), (10) Freire et al. (2011), (11) Jacoby et al. (2005), (12) Thorsett & Chakrabarty (1999).

(PSR 1913+16, see Paper I). Whereas most of the pulsars in double neutron star systems have their mass determined accurately, only a few of the  $\sim 160$  binary pulsars with WD companions have measured masses. These are listed in Table 4. At first sight, a handful of these are more massive than this previous limit of  $1.44 M_{\odot}$ . However, in most of those cases the mass determinations have large uncertainties and in all cases also include mass accreted from the progenitor of their WD companion, i.e. these masses are pulsar masses *after* the recycling phase and not neutron star birth masses after the SN.

To take this effect into account we have estimated upper limits for the birth mass of the neutron star in all systems by subtracting the minimum mass needed to spin up the pulsar using equation (14). The results are shown in the fifth column of Table 4. Since we do not know the true age of the recycled pulsars, nor their braking index, we simply assumed in all cases that the presently observed pulsar spin period,  $P$  is related to their original equilibrium spin period,  $P_{\text{eq}}$  prior to the RLDP via:  $P = \sqrt{2}P_{\text{eq}}$ . For pulsars where the RLDP effect was small the initial spin period after recycling,  $P_0 \simeq P_{\text{eq}}$  and hence  $P \simeq \sqrt{2}P_0$ , which corresponds to the case where the true age is half the characteristic age of a pulsar with braking index  $n = 3$  (see Section 8 for further discussion on braking indices and true ages).

It is possible that some BMSPs have  $P \simeq P_0$  (especially those BMSPs with small values of  $B_0$ ). In this case the neutron star birth masses would be slightly larger than indicated here. However, recall that the limits in Table 4 are absolute upper limits obtained for *idealized* and efficient spin up. Furthermore, once an accreting pulsar reaches its equilibrium

spin period it can still accrete material but the net effect may not be further spin up (depending on the mass-transfer rate,  $\dot{M}$ ). Therefore, it should be emphasized that the actual SN birth mass could in many cases be substantially lower than estimated in Table 4. For example, we have demonstrated in Paper I that PSR J1614–2230 could have accreted  $0.31 M_{\odot}$ , which is substantially more than shown in Table 4 where the pulsar in this case was assumed to be born with a spin period of  $3.15 \text{ ms}/\sqrt{2} = 2.23 \text{ ms}$ , yielding  $\Delta M_{\text{eq}} = 0.09 M_{\odot}$ .

## 10.1 PSR J0621+1002

Considering the derived SN birth masses in Table 4 we notice at first sight in particular PSR J0437–4715 and PSR J0621+1002 as further candidates for pulsars which were potentially born massive ( $\sim 1.7 M_{\odot}$ ), although the error bars are large. Given the uncertainty of the accretion efficiency (i.e. the possible difference between the actual amount of mass accreted and  $\Delta M_{\text{eq}}$ ) we see that in particular PSR J0621+1002 could have been born massive with  $M_{\text{NS,max}}^{\text{birth}} \sim 1.7 M_{\odot}$ . PSR J0621+1002 (Camilo et al. 1996) has an orbital period of 8.3 days and a CO WD companion of mass  $0.67 M_{\odot}$  which is somewhat equivalent to PSR J1614–2230. However, its relatively slow spin period of 28.9 ms and large eccentricity of  $2.5 \times 10^{-3}$  indicate that PSR J0621+1002 did not evolve through an X-ray phase with stable, and relatively long Case A RLO (unlike the situation for PSR J1614–2230). It seems much more evident that PSR J0621+1002 evolved through a rapid, less efficient, mass-transfer phase – such as early Case B RLO (Tauris et al. 2000). In this case the actual amount of accretion must have been at most a few  $10^{-2} M_{\odot}$ . Therefore, its measured mass is very close to its birth mass and *if* future mass measurements of PSR J0621+1002 yield smaller error bars, still centered on its current mass estimate, we conclude that this pulsar belongs to the same class of neutron stars as PSR J1614–2230, Vela X-1 and possibly the Black-Widow pulsar which were all born massive (see Paper I). However, the error bar is quite large and PSR J0621+1002 could turn out to have an ordinary mass of about  $1.4 M_{\odot}$  (the  $2\text{-}\sigma$  lower mass limit).

### 10.1.1 PSR J0437–4715

PSR J0437–4715 is also a potential candidate for a pulsar which could have been born as a neutron star with a mass of  $\sim 1.7 M_{\odot}$ . However, this pulsar has a fairly rapid spin period (like a few other relatively high-mass neutron star candidates in Table 4) which indicates a long spin-up phase. Hence, it may have accreted significantly more than suggested by  $\Delta M_{\text{eq}}$ . In fact, as mentioned before, in the case of PSR J1614–2230 the pulsar might have accreted three times more than suggested by  $\Delta M_{\text{eq}}$ , see fig. 7 in Tauris et al. (2011). The problem is that as soon as the pulsar spin reaches  $P_{\text{eq}}$  (which requires accumulation of mass  $\Delta M_{\text{eq}}$ ) it may remain in near-spin equilibrium and keep accreting on and off while spinning up/down depending on the sign of the accretion torque. The situation is quite different for PSR J0621+1002 which formed through a short lived X-ray phase excluding evolution at near-spin equilibrium for a substantial amount of time. We therefore conclude that

PSR J0437–4715 could originally have been born in a SN with a typical mass of  $\sim 1.4 M_{\odot}$ , even if its present mass is indeed  $\sim 1.76 M_{\odot}$ .

## 11 SUMMARY

We have investigated in detail the recycling process of pulsars with respect to accretion, spin up and the Roche-lobe decoupling phase, and discussed the implications for their spin periods, masses and true ages. In particular, we have discussed the concept of a spin-up line in the  $P\dot{P}$ -diagram and emphasize that such a line cannot be uniquely defined. Besides from the poorly known disk-magnetosphere physics, which introduces large uncertainties, for each individual pulsar the equilibrium spin period,  $P_{\text{eq}}$  also depends on its magnetic inclination angle,  $\alpha$  as well as its accretion history ( $\dot{M}$ ) and its B-field strength. Furthermore, we have applied the Spitkovsky (2006) spin-down torque on radio pulsars which significantly changes the location of the spin-up lines compared to using the vacuum magnetic dipole model, especially for small values of  $\alpha$ .

We have derived a simple analytical expression (equation 14) to evaluate the amount of mass needed to be accreted to spin up a pulsar to any given equilibrium spin period,  $P_{\text{eq}}$ . Our result resembles that of Alpar et al. (1982) and approximately yields the same values (within a factor of two) as the expression derived by Lipunov & Postnov (1984). Using our formula we find, for example, that BMSPs with He WDs and  $P_{\text{eq}} \simeq 2$  ms must have accreted at least  $0.10 M_{\odot}$ , whereas typical BSMPs with CO WDs and  $P_{\text{eq}} \simeq 20$  ms only needed to accrete  $0.005 M_{\odot}$ .

Applying equation (14) enables us to explain the difference in spin distributions between BMSPs with He and CO WDs, respectively. The BMSPs with He WDs often evolved via an X-ray phase with stable RLO on a long timescale, allowing sufficient material to be accreted by the neutron star to spin it up efficiently to a short period, whereas the BMSPs with CO WDs most often have slow spins and evolved from IMXBs which had a short phase of mass transfer via early Case B RLO or Case C RLO – the latter leading to a CE-evolution often followed by Case BB RLO. The only exception known so far is PSR J1614–2230 since this system produced a CO WD orbiting a fully recycled MSP and thus it must have evolved via Case A RLO of an IMXB.

It is not possible to recycle pulsars to become MSPs via wind accretion from  $1.1 - 2.2 M_{\odot}$  post-CE helium stars. However, we have demonstrated that Case BB RLO from such helium stars can spin up pulsars to at least  $\sim 11$  ms. Further studies of these systems are needed.

There is an increasing number of recycled pulsars with WD companions which seem to fall outside the two main populations of BMSPs with He and CO WDs, respectively. These peculiar systems possibly have He WDs and always exhibit slow spin periods between 10 and 100 ms. We suggest that these systems with  $P_{\text{orb}} \geq 1$  day may have formed via Case A RLO of IMXBs. We plan further studies on these binaries.

The Roche-lobe decoupling phase (RLDP), at the terminal stage of the mass transfer (Tauris 2012), has been analysed and we have shown that while the RLDP effect

is important in LMXBs – leading to significant loss of rotational energy of the recycled pulsars as well as characteristic ages at birth which may exceed the age of the Universe – it is not significant in IMXB systems where the duration of the RLDP is short.

In order to track the evolution of pulsars in the  $P\dot{P}$ -diagram we have introduced two types of true age isochrones – one which matches well with the banana shape of the observed distribution of known MSPs. We encourage further statistical population studies to better understand the formation and evolution of radio MSPs in the  $P\dot{P}$ -diagram (see e.g. Kiziltan & Thorsett 2010). The discrepancy between true ages and characteristic spin-down ages of recycled pulsars has been discussed and we confirm that the latter values are completely untrustworthy as true age indicators, leaving WD cooling ages as the only valid, although not accurate, measuring scale (Tauris 2012).

In the combined study presented here and in Paper I we have investigated the recycling of PSR J1614–2230 by detailed modelling of the mass exchanging X-ray phase of the progenitor system. Given the rapid spin of PSR J1614–2230 (3.15 ms) we argue that it is highly unlikely that it evolved through a CE, leaving Case A RLO in an IMXB as the only viable formation channel. We confirm the conclusion from Paper I that the neutron star in PSR J1614–2230 was born massive ( $1.70 \pm 0.15 M_{\odot}$ ). We have demonstrated that PSR J1614–2230 could have been spun-up at  $\dot{M} = \dot{M}_{\text{Edd}}$  and subsequently evolve to its current position in the  $P\dot{P}$ -diagram within 2 Gyr (the estimated cooling age of its white dwarf companion).

Besides PSR J1614–2230, Vela X-1 and possibly the Black-Widow pulsar, we have argued that also PSR J0621+1002 could belong to the same class of neutron stars born massive ( $\geq 1.7 M_{\odot}$ ). The formation of such massive neutron stars in supernovae is in agreement with some supernova explosion models (e.g. Zhang et al. 2008; Ugliano et al. 2012).

## ACKNOWLEDGEMENTS

T.M.T. gratefully acknowledges financial support and hospitality at both the Argelander-Institut für Astronomie, Universität Bonn and the Max-Planck-Institut für Radioastronomie.

## REFERENCES

- Alpar M. A., Cheng A. F., Ruderman M. A., Shaham J., 1982, *Nature*, 300, 728
- Antoniadis J., van Kerkwijk M. H., Koester D., Freire P. C. C., Wex N., Tauris T. M., Kramer M., Bassa C. G., 2012, *ArXiv e-prints*, astro-ph:1204.3948
- Archibald A. M., Stairs I. H., Ransom S. M., Kaspi V. M., Kondratiev V. I., Lorimer D. R., McLaughlin M. A., Boyles J., Hessels J. W. T., Lynch R., van Leeuwen J., Roberts M. S. E., Jenet F., Champion D. J., Rosen R., Barlow B. N., Dunlap B. H., Remillard R. A., 2009, *Science*, 324, 1411
- Backer D. C., Kulkarni S. R., Heiles C., Davis M. M., Goss W. M., 1982, *Nature*, 300, 615

- Bagchi M., 2011, MNRAS, 413, L47
- Bailes M., Bates S. D., Bhalariao V., Bhat N. D. R., Burgay M., Burke-Spolaor S., D'Amico N., Johnston S., Keith M. J., Kramer M., Kulkarni S. R., Levin L., Lyne A. G., Milia S., Possenti A., Spitler L., Stappers B., van Straten W., 2011, Science, 333, 1717
- Bailes M., Harrison P. A., Lorimer D. R., Johnston S., Lyne A. G., Manchester R. N., D'Amico N., Nicastro L., Tauris T. M., Robinson C., 1994, ApJ, 425, L41
- Bassa C. G., van Kerkwijk M. H., Kulkarni S. R., 2003, A&A, 403, 1067
- Bates S. D., Bailes M., Bhat N. D. R., Burgay M., Burke-Spolaor S., D'Amico N., Jameson A., Johnston S., Keith M. J., Kramer M., Levin L., Lyne A., Milia S., Possenti A., Stappers B., van Straten W., 2011, MNRAS, 416, 2455
- Bejger M., Zdunik J. L., Haensel P., Fortin M., 2011, A&A, 536, A92
- Bhalariao V. B., Kulkarni S. R., 2011, ApJ, 737, L1
- Bhat N. D. R., Bailes M., Verbiest J. P. W., 2008, Phys. Rev. D, 77, 124017
- Bhattacharya D., 2002, Journal of Astrophysics and Astronomy, 23, 67
- Bhattacharya D., van den Heuvel E. P. J., 1991, Physics Reports, 203, 1
- Bildsten L., 1998, ApJ, 501, L89
- Bildsten L., Chakrabarty D., Chiu J., Finger M. H., Koh D. T., Nelson R. W., Prince T. A., Rubin B. C., Scott D. M., Stollberg M., Vaughan B. A., Wilson C. A., Wilson R. B., 1997, ApJS, 113, 367
- Bozzo E., Stella L., Vietri M., Ghosh P., 2009, A&A, 493, 809
- Brown G. E., 1995, ApJ, 440, 270
- Burderi L., D'Antona F., Burgay M., 2002, ApJ, 574, 325
- Burderi L., Possenti A., D'Antona F., Di Salvo T., Burgay M., Stella L., Menna M. T., Iaria R., Campana S., d'Amico N., 2001, ApJ, 560, L71
- Callanan P. J., Garnavich P. M., Koester D., 1998, MNRAS, 298, 207
- Camero-Arranz A., Pottschmidt K., Finger M., Wilson-Hodge C. A., Marcu D. M., 2011, ArXiv e-prints, astro-ph:1111.4514
- Camilo F., 1996, in S. Johnston, M. A. Walker, & M. Bailes ed., IAU Colloq. 160: Pulsars: Problems and Progress Vol. 105 of Astronomical Society of the Pacific Conference Series, Intermediate-Mass Binary Pulsars: a New Class of Objects?. pp 539–+
- Camilo F., Lyne A. G., Manchester R. N., Bell J. F., Stairs I. H., D'Amico N., Kaspi V. M., Possenti A., Crawford F., McKay N. P. F., 2001, ApJ, 548, L187
- Camilo F., Nice D. J., Shrauner J. A., Taylor J. H., 1996, ApJ, 469, 819
- Camilo F., Thorsett S. E., Kulkarni S. R., 1994, ApJ, 421, L15
- Campana S., Colpi M., Mereghetti S., Stella L., Tavani M., 1998, A&A Rev., 8, 279
- Canal R., Isern J., Labay J., 1990, ARA&A, 28, 183
- Contopoulos I., Spitkovsky A., 2006, ApJ, 643, 1139
- Corbet R. H. D., 1984, A&A, 141, 91
- Dai H.-L., Li X.-D., 2006, A&A, 451, 581
- D'Amico N., 2000, in M. Kramer, N. Wex, & R. Wielebinski ed., IAU Colloq. 177: Pulsar Astronomy - 2000 and Beyond Vol. 202 of Astronomical Society of the Pacific Conference Series, The Bologna submillisecond pulsar survey. p. 27
- Damour T., Taylor J. H., 1991, ApJ, 366, 501
- D'Angelo C. R., Spruit H. C., 2010, MNRAS, 406, 1208
- D'Angelo C. R., Spruit H. C., 2011, MNRAS, 416, 893
- D'Angelo C. R., Spruit H. C., 2012, MNRAS, 420, 416
- Davidson K., Ostriker J. P., 1973, ApJ, 179, 585
- Deloye C. J., 2008, in C. Bassa, Z. Wang, A. Cumming, & V. M. Kaspi ed., 40 Years of Pulsars: Millisecond Pulsars, Magnetars and More Vol. 983 of American Institute of Physics Conference Series, The Connection Between Low-Mass X-ray Binaries and (Millisecond) Pulsars: A Binary Evolution Perspective. pp 501–509
- Deloye C. J., Bildsten L., 2003, ApJ, 598, 1217
- Demorest P. B., Pennucci T., Ransom S. M., Roberts M. S. E., Hessels J. W. T., 2010, Nature, 467, 1081
- Dewi J. D. M., Podsiadlowski P., Sena A., 2006, MNRAS, 368, 1742
- Dewi J. D. M., Pols O. R., Savonije G. J., van den Heuvel E. P. J., 2002, MNRAS, 331, 1027
- Dewi J. D. M., Tauris T. M., 2000, A&A, 360, 1043
- Dubus G., Lasota J.-P., Hameury J.-M., Charles P., 1999, MNRAS, 303, 139
- Ergma E., Sarna M. J., Antipova J., 1998, MNRAS, 300, 352
- Ferdman R. D., Stairs I. H., Kramer M., McLaughlin M. A., Lorimer D. R., Nice D. J., Manchester R. N., Hobbs G., Lyne A. G., Camilo F., Possenti A., Demorest P. B., Cognard I., Desvignes G., Theureau G., Faulkner A., Backer D. C., 2010, ApJ, 711, 764
- Frank J., King A., Raine D. J., 2002, Accretion Power in Astrophysics: Third Edition. Cambridge University Press
- Freire P. C. C., Abdo A. A., Ajello M., et al. 2011, Science, 334, 1107
- Freire P. C. C., Bassa C. G., Wex N., Stairs I. H., Champion D. J., Ransom S. M., Lazarus P., Kaspi V. M., Hessels J. W. T., Kramer M., Cordes J. M., Verbiest J. P. W., Podsiadlowski P., et al. 2011, MNRAS, 412, 2763
- Geppert U., Urpin V., 1994, MNRAS, 271, 490
- Ghosh P., Lamb F. K., 1979a, ApJ, 232, 259
- Ghosh P., Lamb F. K., 1979b, ApJ, 234, 296
- Ghosh P., Lamb F. K., 1992, in E.P.J. van den Heuvel, S.A. Rappaport ed., X-Ray Binaries and Recycled Pulsars Diagnostics of disk-magnetosphere interaction in neutron star binaries.. Springer, pp 487–510
- Goldreich P., Julian W. H., 1969, ApJ, 157, 869
- Haensel P., Zdunik J. L., 1989, Nature, 340, 617
- Han Z., Podsiadlowski P., Eggleton P. P., 1994, MNRAS, 270, 121
- Hayakawa S., 1985, Phys. Rep., 121, 317
- Hessels J., Ransom S., Roberts M., Kaspi V., Livingstone M., Tam C., Crawford F., 2005, in F. A. Rasio & I. H. Stairs ed., Binary Radio Pulsars Vol. 328 of Astronomical Society of the Pacific Conference Series, Three New Binary Pulsars Discovered With Parkes. p. 395
- Hessels J. W. T., 2008, in Wijnands R., Altamirano D., Soleri P., Degenaar N., Rea N., Casella P., Patruno A., Linares M., eds, American Institute of Physics Conference Series Vol. 1068 of American Institute of Physics Conference Series, The Observed Spin Distributions of Millisecond Radio and X-ray Pulsars. pp 130–134
- Hobbs G., Faulkner A., Stairs I. H., Camilo F., Manchester

- R. N., Lyne A. G., Kramer M., D'Amico N., Kaspi V. M., Possenti A., McLaughlin M. A., Lorimer D. R., Burgay M., Joshi B. C., Crawford F., 2004, *MNRAS*, 352, 1439
- Iben Jr. I., Livio M., 1993, *PASP*, 105, 1373
- Ikhsanov N. R., Beskrovnaya N. G., 2012, *ArXiv e-prints*, astro-ph:1205.2846
- Illarionov A. F., Sunyaev R. A., 1975, *A&A*, 39, 185
- Ivanova N., Justham S., Chen X., De Marco O., et al. 2012, *A&A Rev.*, submitted
- Jacoby B. A., Hotan A., Bailes M., Ord S., Kulkarni S. R., 2005, *ApJ*, 629, L113
- Janssen G. H., Stappers B. W., Kramer M., Nice D. J., Jessner A., Cognard I., Purver M. B., 2008, *A&A*, 490, 753
- Jeffery C. S., Hamann W.-R., 2010, *MNRAS*, 404, 1698
- Kaspi V. M., Johnston S., Bell J. F., Manchester R. N., Bailes M., Bessell M., Lyne A. G., D'Amico N., 1994, *ApJ*, 423, L43
- Keith M. J., Jameson A., van Straten W., Bailes M., Johnston S., Kramer M., Possenti A., Bates S. D., Bhat N. D. R., Burgay M., Burke-Spolaor S., D'Amico N., Levin L., McMahon P. L., Milia S., Stappers B. W., 2010, *MNRAS*, 409, 619
- Kippenhahn R., Weigert A., 1990, *Stellar Structure and Evolution*. Springer, Berlin
- Kiziltan B., Thorsett S. E., 2010, *ApJ*, 715, 335
- Kluzniak W., Ruderman M., Shaham J., Tavani M., 1988, *Nature*, 334, 225
- Konar S., Bhattacharya D., 1997, *MNRAS*, 284, 311
- Kramer M., Lyne A. G., O'Brien J. T., Jordan C. A., Lorimer D. R., 2006, *Science*, 312, 549
- Kuijken K., Gilmore G., 1989, *MNRAS*, 239, 605
- Lamb F. K., Pethick C. J., Pines D., 1973, *ApJ*, 184, 271
- Langer N., 1989, *A&A*, 210, 93
- Lattimer J. M., Yahil A., 1989, *ApJ*, 340, 426
- Lewin W. H. G., van der Klis M., 2006, *Compact stellar X-ray sources*. Cambridge University Press
- Li J., Wickramasinghe D. T., 1998, *MNRAS*, 300, 1015
- Li X.-D., 2002, *ApJ*, 564, 930
- Lin J., Rappaport S., Podsiadlowski P., Nelson L., Paxton B., Todorov P., 2011, *ApJ*, 732, 70
- Lipunov V. M., Postnov K. A., 1984, *Ap&SS*, 106, 103
- Locsei J. T., Melatos A., 2004, *MNRAS*, 354, 591
- Lorimer D. R., Faulkner A. J., Lyne A. G., Manchester R. N., Kramer M., McLaughlin M. A., Hobbs G., Possenti A., Stairs I. H., Camilo F., Burgay M., D'Amico N., Corongiu A., Crawford F., 2006, *MNRAS*, 372, 777
- Manchester R. N., Hobbs G. B., Teoh A., Hobbs M., 2005, *AJ*, 129, 1993
- Manchester R. N., Taylor J. H., 1977, *Pulsars*. W. H. Freeman, San Francisco
- Michel F. C., 1991, *Theory of neutron star magnetospheres*. The University of Chicago Press
- Miyaji S., Nomoto K., Yokoi K., Sugimoto D., 1980, *PASJ*, 32, 303
- Nagase F., 1989, *PASJ*, 41, 1
- Navarro J., de Bruyn A. G., Frail D. A., Kulkarni S. R., Lyne A. G., 1995, *ApJ*, 455, L55+
- Nelson L. A., Dubeau E., MacCannell K. A., 2004, *ApJ*, 616, 1124
- Nelson R. W., Bildsten L., Chakrabarty D., Finger M. H., Koh D. T., Prince T. A., Rubin B. C., Scott D. M., Vaughan B. A., Wilson R. B., 1997, *ApJ*, 488, L117
- Nice D. J., Splaver E. M., Stairs I. H., 2003, in M. Bailes, D. J. Nice, & S. E. Thorsett ed., *Radio Pulsars Vol. 302 of Astronomical Society of the Pacific Conference Series, Neutron Star Masses from Arecibo Timing Observations of Five Pulsar-White Dwarf Binary Systems*. pp 75+
- Nice D. J., Stairs I. H., Kasian L. E., 2008, in C. Bassa, Z. Wang, A. Cumming, & V. M. Kaspi ed., *40 Years of Pulsars: Millisecond Pulsars, Magnetars and More Vol. 983 of American Institute of Physics Conference Series, Masses of Neutron Stars in Binary Pulsar Systems*. pp 453-458
- Nomoto K., 1984, *ApJ*, 277, 791
- Paczynski B., 1976, in P. Eggleton, S. Mitton, & J. Wheeler ed., *Structure and Evolution of Close Binary Systems Vol. 73 of IAU Symposium, Common Envelope Binaries*. Dordrecht, Holland, pp 75+
- Passy J.-C., De Marco O., Fryer C. L., Herwig F., Diehl S., Oishi J. S., Mac Low M.-M., Bryan G. L., Rockefeller G., 2012, *ApJ*, 744, 52
- Patruno A., 2010, *ArXiv astro-ph/1007.1108*
- Patruno A., Watts A. L., 2012, in T. Belloni, M. Mendez ed., *Timing Neutron Stars: Pulsations, Oscillations and Explosions Astrophysics and Space Science, Springer, Accreting Millisecond X-ray Pulsars*
- Phinney E. S., 1992, *Royal Society of London Philosophical Transactions Series A*, 341, 39
- Phinney E. S., Kulkarni S. R., 1994, *ARA&A*, 32, 591
- Podsiadlowski P., 1991, *Nature*, 350, 136
- Podsiadlowski P., 2001, in P. Podsiadlowski, S. Rappaport, A. R. King, F. D'Antona, & L. Burderi ed., *Evolution of Binary and Multiple Star Systems Vol. 229 of Astronomical Society of the Pacific Conference Series, Common-Envelope Evolution and Stellar Mergers*. pp 239+
- Podsiadlowski P., Langer N., Poelarends A. J. T., Rappaport S., Heger A., Pfahl E., 2004, *ApJ*, 612, 1044
- Podsiadlowski P., Rappaport S., Pfahl E. D., 2002, *ApJ*, 565, 1107
- Pringle J. E., 1981, *ARA&A*, 19, 137
- Pringle J. E., Rees M. J., 1972, *A&A*, 21, 1
- Pylyser E., Savonije G. J., 1988, *A&A*, 191, 57
- Pylyser E. H. P., Savonije G. J., 1989, *A&A*, 208, 52
- Radhakrishnan V., Srinivasan G., 1982, *Current Science*, 51, 1096
- Rappaport S., Podsiadlowski P., Joss P. C., Di Stefano R., Han Z., 1995, *MNRAS*, 273, 731
- Rappaport S. A., Fregeau J. M., Spruit H., 2004, *ApJ*, 606, 436
- Ruderman M., Shaham J., Tavani M., 1989, *ApJ*, 336, 507
- Shapiro S. L., Teukolsky S. A., 1983, *Black holes, white dwarfs, and neutron stars: The physics of compact objects*. Wiley-Interscience, New York
- Shibazaki N., Murakami T., Shaham J., Nomoto K., 1989, *Nature*, 342, 656
- Shklovskii I. S., 1970, *Soviet Ast.*, 13, 562
- Spitkovsky A., 2006, *ApJ*, 648, L51
- Spitkovsky A., 2008, in C. Bassa, Z. Wang, A. Cumming, & V. M. Kaspi ed., *40 Years of Pulsars: Millisecond Pulsars, Magnetars and More Vol. 983 of American Institute of Physics Conference Series, Pulsar Magnetosphere: The Incredible Machine*. pp 20-28
- Splaver E. M., Nice D. J., Stairs I. H., Lommen A. N.,

- Backer D. C., 2005, *ApJ*, 620, 405
- Spruit H. C., Taam R. E., 1993, *ApJ*, 402, 593
- Srinivasan G., Bhattacharya D., Muslimov A. G., Tsygan A. J., 1990, *Current Science*, 59, 31
- Stairs I. H., Faulkner A. J., Lyne A. G., Kramer M., Lorimer D. R., McLaughlin M. A., Manchester R. N., Hobbs G. B., Camilo F., Possenti A., Burgay M., D'Amico N., Freire P. C., Gregory P. C., 2005, *ApJ*, 632, 1060
- Taam R. E., van den Heuvel E. P. J., 1986, *ApJ*, 305, 235
- Tauris T. M., 1996, *A&A*, 315, 453
- Tauris T. M., 2011, in Schmidtobreick L., Schreiber M. R., Tappert C., eds, *Evolution of Compact Binaries Vol. 447 of Astronomical Society of the Pacific Conference Series, Five and a Half Roads to Form a Millisecond Pulsar*. p. 285
- Tauris T. M., 2012, *Science*, 335, 561
- Tauris T. M., Langer N., Kramer M., 2011, *MNRAS*, 416, 2130
- Tauris T. M., Savonije G. J., 1999, *A&A*, 350, 928
- Tauris T. M., Sennels T., 2000, *A&A*, 355, 236
- Tauris T. M., van den Heuvel E. P. J., 2006, *Formation and evolution of compact stellar X-ray sources*. Cambridge University Press, pp 623–665
- Tauris T. M., van den Heuvel E. P. J., Savonije G. J., 2000, *ApJ*, 530, L93
- Thorsett S. E., Chakrabarty D., 1999, *ApJ*, 512, 288
- Ugliko M., Janka H.-T., Marek A., Arcones A., 2012, *ArXiv e-prints*, astro-ph:1205.3657
- Van Den Heuvel E. P. J., Bitzaraki O., 1994, *Mem. Soc. Astron. Italiana*, 65, 237
- van der Klis M., 2006, *Rapid X-ray Variability*. Cambridge University Press, pp 39–112
- van der Sluys M. V., Verbunt F., Pols O. R., 2005, *A&A*, 431, 647
- van Haften L. M., Nelemans G., Voss R., Jonker P. G., 2012, *A&A*, 541, A22
- van Haften L. M., Nelemans G., Voss R., Wood M. A., Kuijpers J., 2012, *A&A*, 537, A104
- van Kerkwijk M. H., Bassa C. G., Jacoby B. A., Jonker P. G., 2005, in F. A. Rasio & I. H. Stairs ed., *Binary Radio Pulsars Vol. 328 of Astronomical Society of the Pacific Conference Series, Optical Studies of Companions to Millisecond Pulsars*. pp 357–+
- van Kerkwijk M. H., Chakrabarty D., Pringle J. E., Wijers R. A. M. J., 1998, *ApJ*, 499, L27
- van Paradijs J., 1996, *ApJ*, 464, L139+
- Vasyliunas V. M., 1979, *Space Sci. Rev.*, 24, 609
- Verbiest J. P. W., Bailes M., van Straten W., Hobbs G. B., Edwards R. T., Manchester R. N., Bhat N. D. R., Sarkissian J. M., Jacoby B. A., Kulkarni S. R., 2008, *ApJ*, 679, 675
- Wang J., Zhang C. M., Zhao Y. H., Kojima Y., Yin H. X., Song L. M., 2011, *A&A*, 526, A88
- Wang Y.-M., 1997, *ApJ*, 475, L135+
- Webbink R. F., Rappaport S., Savonije G. J., 1983, *ApJ*, 270, 678
- Wellstein S., Langer N., 1999, *A&A*, 350, 148
- Wijnands R., van der Klis M., 1998, *Nature*, 394, 344
- Wolszczan A., Doroshenko O., Konacki M., Kramer M., Jessner A., Wielebinski R., Camilo F., Nice D. J., Taylor J. H., 2000, *ApJ*, 528, 907
- Worley A., Krastev P. G., Li B., 2008, *ApJ*, 685, 390
- Yi I., Wheeler J. C., Vishniac E. T., 1997, *ApJ*, 481, L51
- Zhang C. M., Kojima Y., 2006, *MNRAS*, 366, 137
- Zhang W., Woosley S. E., Heger A., 2008, *ApJ*, 679, 639

## APPENDIX A: IDENTIFYING THE NATURE OF A PULSAR COMPANION STAR

For stellar evolutionary purposes, and for observers to judge the possibilities to detect a companion, it would be useful to have a tool to predict the most likely nature of the companion star of a given binary pulsar. As discussed in Section 3 radio pulsars are presently found with the following companions:

- Main sequence stars – *MS*
- Neutron stars – *NS*
- CO/ONeMg white dwarfs – *CO*
- He white dwarfs – *He*
- Ultra-light companions (or planets) – *UL*

Although still not detected, radio pulsars are also expected to exist in systems with either:

- Helium stars – *HS*
- (sub)Giant stars – *GS*
- Black Holes – *BH*

As explained in Section 3 pulsar systems found in globular clusters are not useful as probes of stellar evolution due to perturbations in their dense environment. We shall denote the companions of such pulsars by:

- Globular cluster companions – *GC*

The usual characteristic parameters measured of an observed binary pulsar are: the spin period ( $P$ ), the period derivative ( $\dot{P}$ ), the orbital period ( $P_{\text{orb}}$ ) and the projected semi-major axis of the pulsar ( $a_1$ ). From the latter two parameters one can calculate the mass function ( $f$ ) which is needed, but not sufficient, to estimate the mass of the companion star ( $M_2$ ). Furthermore, in many cases it is also possible to estimate the eccentricity ( $ecc$ ). Based on these parameters we state simple conditions in Table A1 which can be used to identify the most likely nature of pulsar companions at the 95 per cent level of confidence (based on statistics from current available data). These conditions can be directly applied to the online, public available *ATNF Pulsar Catalogue*, <http://www.atnf.csiro.au/research/pulsar/psrcat/> (Manchester et al. 2005) in order to select a subsample of pulsars with certain companion stars.

One example of the few pulsars where the identification fails is PSR J1614–2230 given its unusual combination of being fully recycled and having a CO WD companion, as discussed in this paper. The identification conditions can in principle be optimised further to increase the level of confidence even more. However, this would not only require these conditions to be updated frequently with new discoveries of somewhat peculiar binary pulsars but also lead to undesirable complexity in the conditions. The main uncertainty factor is the (most often) unknown orbital inclination angle of the binary system. The transition between systems with *UL* and *He* companions and, in particular, between *He* and *CO* companions is difficult to define satisfactorily. Furthermore, WD+NS systems where the last formed compact object is the neutron star are very difficult to distinguish from NS+NS systems, *if* based solely on data from the last formed (non-recycled) NS. Finally, we note that the long-sought after radio pulsar in a binary with a black hole companion

(NS+BH or BH+NS) will most likely be mildly recycled (i.e. NS+BH) due to its much longer lifetime as an observable pulsar after accretion. In this case it may be difficult to distinguish it from a system where the pulsar has a *NS* companion orbiting with a small inclination angle. On the other hand, if the pulsar is not recycled then such a BH+NS system could resemble a pulsar with an (undetected) *MS* companion.

**Table A1.** The most likely nature of a radio pulsar companion star based on observable characteristics. The selection conditions can be directly applied to the *ATNF Pulsar Catalogue* (Manchester et al. 2005). See also Section 3 for further discussions.

Companion type	Conditions
<i>MS</i>	$M_2^* > 0.5 M_\odot$ and $P_{\text{orb}} > 50^{\text{d}}$
<i>NS</i>	$P_{\text{orb}} < 50^{\text{d}}$ and $ecc > 0.05$
<i>CO</i>	$M_2^* > 0.335 M_\odot$ and $P_{\text{orb}} < 75^{\text{d}}$ and $ecc < 0.05$ and $P > 8$ ms
<i>He</i>	$M_2^* > 0.08 M_\odot$ and $\{(P_{\text{orb}} < 75^{\text{d}}$ and $M_2^* < 0.335 M_\odot\}$ or $(P_{\text{orb}} > 75^{\text{d}}$ and $M_2^* < 0.46 M_\odot)\}$
<i>UL**</i>	$M_2^* < 0.08 M_\odot$

\* The median companion mass  $M_2$  is calculated for an orbital inclination angle  $i = 60^\circ$  and an assumed pulsar mass  $M_{\text{NS}} = 1.35 M_\odot$ .\*\* Many pulsars with unmeasured values of  $a_1$  are also expected to host an ultra-light companion if  $P_{\text{orb}} < 2$  days and  $P < 8$  ms.